平成２１年６月１６日 安全対策調査会	平成２１年２月６日 タミフル基礎WG
資料2－2	資料1

リン酸オセルタミビルの基礎的調査検討のための主要な文献等

・Effect of a neuraminidase inhibitor (oseltamivir) on mouse jump-down behavior via stimulation of dopamin receptors

Minoru Suzuki and Yutaka Masuda, Biomedical Research 29(5) 233-238, 2008・・・・・p1

・Activation of the prodrug oseltamivir is impaired by two newly identified carboxylesterase 1 variants

Hao-Jie Zhu and John S. Markowitz, Drug Metab Dispos doi:10.1124/dmd.108.024943, 2008・・・・・p7

・Limited brain distribution of Ro 64-0802, a pharmacologically active form of oseltamivir, by active efflux across the blood brain barrier mediated by organic anion transporter 3 and multidrug resistance-associated protein 4

Atsushi Ose, Mototsugu Ito, et al. Drug Metab Dispos 2008; doi:10.1124/dmd.108.024018 (2008)・・・・・p11

・Human carboxylesterases HCE1 and HCE 2: Ontogenic expression, inter-individual variability and differential hydrolysis of oseltamivir, aspirin, deltamethirin and permethirin.

Yang, et al. Biochem Pharmacol 2008 ; doi:10.1016/j.bcp.2008.10.005・・・・・p18

・異常行動モデルとしての薬物誘発ジャンピング行動に対するタミフルの影響とその防御法に関する研究

小野ら （第 113 回日本薬理学会近畿支部会）・・・・・p28

以上

Biomedical Research 29 (5) 233-238, 2008

Effect of a neuraminidase inhibitor (oseltamivir) on mouse jump-down behavior via stimulation of dopamine receptors

Minoru SUZUKI[1] and Yutaka MASUDA[2]
[1]Department of Neuropsychiatry, [2]Psychosomatic Division, Akita University School of Medicine, Akita 010-8543, Japan
(Received 7 July 2008; and accepted 31 July 2008)

ABSTRACT

Oseltamivir (Tamiflu®, Roche Laboratories, Inc.) is a neuraminidase inhibitor that can cause jump-down behaviors in children. There is a mouse slip-down model, in which the dopamine D2 receptor activity is increased by serum sialoglycolipids and the mouse jump-down behavior appears in response to the dopamine D2 receptor agonist, PPHT. The present study examined the effect of oseltamivir on jump-down behavior in mice. Oseltamivir sialylates a serum glycolipid and this modified glycolipid induces jump-down behavior via the stimulation of dopamine D2 receptors. This mechanism may be involved in the abnormal behavior of children taking oseltamivir.

Oseltamivir (Tamiflu®, Roche Laboratories, Inc.) is an antiviral drug used to treat influenza. It can reduce the duration and severity of the illness if administered within 48 hours after the onset of symptoms (4, 13, 19). Recently, fatal accidents due to abnormal behaviors such as jumping from high places after taking oseltamivir have been reported in juvenile patients in Japan (7, 18, 20). These abnormal behaviors usually occur after the initial administration of oseltamivir (8). In March 2007, the Japanese Ministry of Health, Labour and Welfare announced a ban on the use of oseltamivir in patients from 10–19 years of age (12). However, little is known about either the contribution of this drug to these behaviors or the mechanism involved.

Sialic acids exist mostly in the terminal positions of biomolecules (such as glycoproteins, glycolipids and gangliosides) and cell membranes and are involved in a wide variety of physiological processes, including immune functions (24, 26). Neuraminidases are called sialidases because they hydrolyze the terminal sialic acid linkage in these biomolecules and variations in human sialidase activity have been implicated in serious diseases and symptoms including neuropsychiatric problems (1, 2, 25). Oseltamivir is a representative neuraminidase inhibitor.

Slip-down behavior in mice is induced by a comparatively low-dose of the dopamine D2 receptor agonist, PPHT (17), and that the representative dopamine D2 receptor agonists morphine and quinpirole induce jump-down behavior in mice (6, 10). In addition, we noticed that mouse jump-down behavior appeared by increased doses of PPHT during previous experiment. An increase in dopamine D2 receptor activity is closely associated with sialylation of a serum glycolipid (15). Oseltamivir might influence the dopamine D2 receptor activity through sialoglycolipids and oseltamivir might be connected to the manifestation of the jump-down behavior. An animal model is useful for understanding these behavioral phenomena. Therefore, the jump-down behavior in mice could be a model for the jump-down behavior in human children taking oseltamivir.

The present study investigated the effect of oseltamivir on jump-down behavior in mice, a serum glycolipid associated with this behavior and changes in glycosylation of this glycolipid in response to oseltamivir.

Address correspondence to: Minoru Suzuki M.D., Department of Neuropsychiatry, Akita University School of Medicine, 1-1-1 Hondo, Akita 010-8543, Japan
Tel: +81-18-834-1111, Fax: +81-18-884-6445
E-mail: suzukimi@kyusei.or.jp

MATERIALS AND METHODS

Animals. Eight-week-old male ddY mice that weighed 25–30 g were purchased from Japan SLC (Shizuoka, Japan). A group of 5 mice were housed in a plastic cage (338 × 140 × 225 mm) with free access to food (ED-7; Clea Japan, Tokyo, Japan) and water. The animal room was kept at 21–25°C with 50–60% humidity and was illuminated from 7 : 00 to 19 : 00. All experiments were carried out according to the guidelines of the Ethics Committee for Animal Experiments of the Akita University School of Medicine.

Dosage of PPHT inducing mouse jump-down behavior. The dopamine D2 receptor agonist 2-(*N*-phenylethyl-*N*-propyl) amino-5-hydroxytetralin hydrochloride (PPHT; Funakoshi, Tokyo, Japan) was dissolved in water. The observation of mouse jump-down behavior is the same as procedure of observation of mouse slip-down behavior which we previously reported (17). This method was established for the detection of neuronal D2 dopamine receptor activity. In brief, a raised platform measuring 10 cm in diameter and 20 cm high was prepared. One group of five mice in a cage was intraperitoneally injected with 200, 150, 100, or 50 μg/kg of PPHT, or 100 μL of physiological saline (PS) as a control. Twenty minutes after the injection, the mice were placed individually on the platform for 5 min and thereafter both slip-down behavior and jump-down behavior were investigated.

Effect of oseltamivir on jump-down behavior. From results of the above experiment, 50 μg/kg of PPHT was determined to be a suboptimal dose of mouse jump-down behavior. Other naïve mice groups were prepared. Two trials separated by a 20-min interval were observed to confirm that all of the mice remained on the platform for 5 min without jumping-down and slipping-down before the administration of drugs. Then the mice were injected intraperitoneally with oseltamivir solution or with PS as a control (5 mice each). Oseltamivir was dissolved in water and 25 mg/kg, 50 mg/kg, or 100 mg/kg was injected intraperitoneally in mice (5 mice each). Two hours after injection with oseltamivir solution or with PS, each mouse was placed individually on the platform and jump-down behavior was examined for 5 min. These mice were also injected intraperitoneally with PPHT at the suboptimal dose of 50 μg/kg. Twenty minutes after injection with PPHT of 50 μg/kg, jump-down behavior was again examined for 5 min.

Isolation of the glycolipid fraction from sera. The effect of oseltamivir was thought to be related to serum glycolipid. Oseltamivir solution (100 mg/kg) was injected intraperitoneally in 5 groups of mice and PS (100 μL) was injected into another 5 groups. Sera were collected 2 h after this treatment. Glycolipids were separated from the sera by the methanol-chloroform method, as reported previously (16). In brief, 1 mL of sera was added to 2.5 mL methanol and 1.25 mL chloroform. The fluid was agitated for 2 min and left at room temperature (RT) for 10 min. Then another 1.25 mL chloroform was added and the mixture was agitated for 30 s. After addition of 1.25 mL water and agitation for another 30 s, the mixture was centrifuged at 150 × *g* for 5 min at RT, thus resulting in an upper methanol-water layer containing proteins and a lower chloroform layer containing lipids and glycolipids. The lower layer was collected and evaporated and the lipids and glycolipids were redissolved in 2 mL water. The solution was applied to an ion-exchange DE-52 column (Whatman International, Maidstone, UK) saturated with 10 mM $NaHCO_3$, pH 8.3 and eluted with 50, 100, 150, 200, 250 and 300 mM NaCl in stages. The eluted fractions were refined to less than 3 kDa with the use of an ultrafiltration membrane (Centricon; Amicon, Tokyo, Japan). Two hundred microliters of each fraction was injected intraperitoneally into the naïve group of 5 mice and then the mice were additionally injected with 50 μg/kg PPHT 20 min after the fraction injection. The effect on neural D2 receptor activity was investigated by the jump-down method.

Detection of the sugar chain structures of effective glycolipids. To detect the sugar chain structures of the glycolipids, a 50% ethanol lectin-enzyme-linked immunosorbent assay (lectin-ELISA) was performed, as reported previously (16). In brief, 50 μL of the lipid fraction eluted with 250 mM NaCl in the serum of 5 mice treated with 100 mg/kg oseltamivir or 5 mice treated with PS was mixed with 50 μL ethanol and poured into one well of a 96-well plate (Sumitomo Bakelite, Tokyo, Japan). After 2 h, the well was washed three times with a washing solution (PS containing 0.005% Tween 20; Seikagaku Co., Tokyo, Japan). After a 30-min block with 5% bovine serum albumin (Sigma-Aldrich, St. Louis, MO), the well was washed again three times with the same washing solution. Five different biotinylated lectins that recognize specific sugar

chain structures (ABA, Galβ$_{1-3}$GalNAc; DBA, GalNAcα$_{1-3}$GalNAc; SSA, Sialα$_{2-6}$Gal; AAL, Fucα$_{1-2}$Gal; MAM, Sialα$_{2-3}$Gal) were prepared at 2 μg/mL in PS and 100 μL of the mixture was added to the well. After 1 h incubation at RT, the well was washed three times with the washing solution. One hundred microliters of peroxidase-conjugated avidin (Seikagaku Co.) prepared at 0.1 μg/mL in PS was then added to the well. After 15-min incubation at RT, the well was washed four times with PS. Development of the color reaction was performed with a developing kit (Sumitomo Bakelite) and absorbance was measured at 455 nm and 650 nm.

Confirmation of the glycolipid effect. The glycolipid fraction eluted with 250 mM NaCl from the sera of mice treated with PS or the sera of mice treated with 100 mg/kg oseltamivir was applied to a Maackia amurensis agglutinin (MAM) affinity column (Seikagaku Co.). MAM is the specific lectin for Sialα$_{2-3}$Gal and this affinity column was used to refine the glycolipid that has Sialα$_{2-3}$Gal in the sugar chain terminal. Fractions eluted with 6 M urea were desalted over a CD-50 desalting column (Pharmacia, Uppsala, Sweden) and freeze-dried. Glycolipids were redissolved in water to a concentration of 10 μg/mL. A concentration of 25, 50, or 100 μg/kg of glycolipid solution was injected intraperitoneally into mice (5 each) and the effect on jump-down behavior was investigated after treatment with the suboptimal dose of PPHT.

Statistical analysis. The Kruskal-Wallis rank test was used to determine significant differences among groups. The Mann-Whitney U test was used for further analysis. $P < 0.01$ was considered to be statistically significant.

RESULTS

Suboptimal dose of the dopamine D2 receptor agonist PPHT

A concentration of 100 μg/kg of PPHT induced slip-down behavior, but 50 μg/kg did not. On the other hand, concentrations of 200 and 150 μg/kg induced jump-down behavior, but 100 and 50 μg/kg did not (Table 1).

Effect of oseltamivir on jump-down behavior

To determine whether oseltamivir induces jump-down behavior in mice, the behavior of the mice 2 h were examined after the injection of various concentrations of oseltamivir or PS and then at 20 min after the injection of 50 μg/kg PPHT. Mice treated with oseltamivir or PS showed no jump-down behavior, but after being treated with D2 receptor agonist, the mice treated with 50 or 100 mg/kg oseltamivir showed jump-down behavior (Table 2). The number of mice exhibiting jump-down behavior increased dose-dependently.

Effects of serum glycolipid fractions on jump-down behavior

To determine whether glycolipid fractions from 100 mg/kg oseltamivir-treated mice induce jump-down behavior, the mice were injected intraperitone-

Table 1 *Jump-down or slip-down behavior induced by the dopamine D2 receptor agonist PPHT*

	Dose of PPHT (μg/kg)				PS
	200	150	100	50	(control)
Jump-down behavior	5	5	0	0	0
Slip-down behavior	0	0	5	0	0

Values in this table indicate the number of mice that showed jump-down or slip-down behavior among the 5 treated mice. PPHT: 2-(*N*-phenylethyl-*N*-propyl) amino-5-hydroxytetralin hydrochloride. PS: physiologic saline.

Table 2 *Number of mice exhibiting jump-down behavior*

	Dose of oseltamivir solution (mg/kg)			PS
	100	50	25	(control)
2 h after oseltamivir injection	0	0	0	0
20 min after further D2 receptor agonist injection	5*	2*	0	0

Values in this table indicate the number of mice that showed jump-down behavior among the 5 treated mice. The D2 receptor agonist was used at 50 μg/kg. In the lower data, a statistically significant difference was found ($k = 3$, $n_1 = n_2 = n_3 = 5$, $n = 15$, $H = 12.5$, $P \leq 0.009$; Kruskal-Wallis rank test). *$P < 0.01$ vs. control (Mann-Whitney U test). PS: physiologic saline.

ally with serum glycolipid fractions eluted with various concentrations of NaCl and evaluated their behavior. The glycolipid fraction from 100 mg/kg oseltamivir-treated mice eluted with 250 mM NaCl induced jump-down behavior (Table 3). None of the other fractions from 100 mg/kg oseltamivir- or PS-treated mice induced this behavior.

Sugar chain reactivities of glycolipid eluted with 250 mM NaCl

To identify the sugar chain structures of the effective glycolipid eluted with 250 mM NaCl, the reactivity of five kinds of sugar chain structures were investigated using by the 50% ethanol lectin-ELISA method. The sugar chain structures Galβ$_{1-3}$GalNAc, GalNAcα$_{1-3}$GalNAc, Sialα$_{2-6}$Gal and Sialα$_{2-3}$Gal were found in the glycolipid fractions of mice treated with 100 mg/kg oseltamivir or PS (Table 4). No Fucα$_{1-2}$Gal reactivity was found. The Galβ$_{1-3}$GalNAc, GalNAcα$_{1-3}$GalNAc and Sialα$_{2-6}$Gal reactivity was similar in both groups, but the Sialα$_{2-3}$Gal reactivity was greater in the mice treated with 100 mg/kg oseltamivir than in the mice treated with PS.

Confirmation of the glycolipid effect

To confirm the glycolipid effect, three concentrations of the glycolipid fraction or PS were each injected intraperitoneally into 5 mice and the effects on jump-down behavior were investigated. After refinement with a MAM column, the glycolipid from mice treated with oseltamivir dose-dependently induced jump-down behavior after treatment with 50 μg/kg PPHT. The glycolipid from mice treated with PS did not induce this behavior, even at the dose of 100 μg/kg and after treatment with 50 μg/kg PPHT (Table 5).

DISCUSSION

Oseltamivir is a sialic acid analogue that inhibits influenza type A and type B neuraminidase, the viral enzyme that allows the release of virus from infected cells. In addition, oseltamivir is an ester prodrug activated by hepatic carboxylesterases. It is thought that the sudden onset of reactions such as abnormal behaviors and sudden death during sleep are caused by the prodrug of oseltamivir, oseltamivir phosphate. On the other hand, adverse reactions such as

Table 3 *Jump-down behavior in mice treated with glycolipids isolated from sera*

Injected fraction	Serum glycolipids from mice treated with PS	Serum glycolipids from mice treated with 100 mg/kg oseltamivir
Eluted with 50 mM NaCl	0	0
100	0	0
150	0	0
200	0	0
250	0	5
300	0	0

Values in this table indicate the number of mice that showed jump-down behavior among the 5 injected mice. All mice were also treated with 50 μg/kg dopamine D2 receptor agonist PPHT 20 min after the fraction injection. PS: physiologic saline.

Table 4 *Sugar chain reactivities of the serum glycolipids eluted with 250 mM NaCl*

	Serum glycolipid from mice treated with PS	Serum glycolipid from mice treated with 100 mg/kg oseltamivir	PS (negative control)
Galβ$_{1-3}$GalNAc	0.126	0.127	0.036
GalNAcα$_{1-3}$GalNAc	0.116	0.118	0.050
Sialα$_{2-6}$Gal	0.091	0.088	0.045
Sialα$_{2-3}$Gal	0.086	0.153	0.043
Fucα$_{1-2}$Gal	0.037	0.035	0.036

Values indicate absorbance at dual wavelengths of 455 nm and 650 nm.
Serum glycolipid was obtained from the 5 mice treated with PS or the 5 mice treated with 100 mg/kg oseltamivir.
PS: physiologic saline.

Table 5 *Mice jumping-down after treatment with refined glycolipid*

Glycolipid dose (μg/kg)	Glycolipid from mice treated with PS	Glycolipid from mice treated with 100 mg/kg oseltamivir
100	0	5*
50	0	3
25	0	0
PS (control)	0	

Values in this table indicate the number of mice that showed jump-down behavior among 5 treated mice. All mice were treated with 50 μg/kg D2 receptor agonist. In the right column data, statistical differences were analyzed by the Kruskal-Wallis rank test ($k=3$, $n_1=n_2=n_3=5$, $n=15$, $H=12.5$, $P<0.009$).

*$P<0.01$ vs. control (Mann-Whitney U test). PS: physiologic saline.

pneumonia, sepsis, hyperglycemia and gastrointestinal bleeding are thought to be delayed reactions induced by oseltamivir and the active metabolite of oseltamivir, oseltamivir carboxylate (OC), is thought to be the cause of delayed reactions (9). Recently, OC has been described to have an inhibitory action on human cytosolic sialidase. It was hypothesized that this effect might be a mechanism by which oseltamivir induces adverse neuropsychiatric reactions (14). Since OC inhibits the human cytosolic sialidase and it can also damage the cell functions in various human tissues, this may explain the delayed reactions induced by oseltamivir. However, abnormal behaviors occur after the initial administration of oseltamivir (8), therefore, it is supposed that the mechanism of such abnormal behavior might be different from the hypothesis (9).

There were two novel findings in the present study: 1) oseltamivir induced jump-down behavior in mice in association with stimulated neuronal D2 receptor activity and 2) this effect of oseltamivir was associated with the Sialα_{2-3}Gal form of sialylation of serum glycolipid. Neither oseltamivir nor its carboxylic acid metabolite, GS4071, influence the re-uptake/release of three monoamines (dopamine, serotonin and norepinephrine) or GTP binding in postsynapses (23). However, another investigation using rats indicates the possibility that oseltamivir has effects on the central nervous system, especially when combined with other agents (11). Serum glycolipid would be expected to be sialylated following oseltamivir treatment; however, the mechanism of sialylation with the Sialα_{2-3}Gal form is not clear. Lipids can pass through the blood-brain barrier and dopaminergic neurons possess glycoside receptors (21). Serum glycolipid regulates the dopaminergic neuron activity, while sialylation enhances the effect of increased D2 receptor activity by agonists. A previous study reported that oseltamivir enhances the effect of ganglioside on opioid receptors (5).

Hyperthermia excites the hypothalamus, which decreases the plasma sialic acid level (3). Decreased sialylation of serum glycolipids regulates dopaminergic neuron activity relating to hyperthermia. With regard to the jump-down behavior of children taking oseltamivir, oseltamivir may block glycolipid desialylation and neuronal D2 receptor activity in children infected with influenza may be increased. Slip-down behavior in mice is caused by dopaminergic hyperactivity to escape from an uneasy situation (15). Jump-down behavior in mice is also caused by dopaminergic hyperactivity and could also indicate behavior to escape from an uneasy situation. This is a basic adaptative behavior in animals and experience refines the behavior. Some children may not be able to handle this type of hyperactive D2 activity.

The results of the present study shed light on the mechanism underlying abnormal behaviors of some children in response to oseltamivir. It would be useful to examine the oseltamivir-induced jump-down behavior in influenza-infected mice. Human studies such as a sugar-chain analysis of blood phospholipids of patients who take oseltamivir are also needed.

REFERENCES

1. Becker CG, Artola A, Gerardy-Schahn R, Becker T, Welzl H and Schachner M (1996) The polysialic acid modification of the neural cell adhesion molecule is involved in spatial learning and hippocampal long-term potentiation. *J Neurosci Res* 45, 143–152.
2. Boyzo A, Ayala J, Gutiérrez R and Hernández-R J (2003) Neuraminidase activity in different regions of the seizing epileptic and non-epileptic brain. *Brain Res* 964, 211–217.
3. Chen WF, Chen JJ and Chen L (1995) Excitation of hypothalamic nucleus arcuatus neuron induced decrease of plasma

sialic acid level in rats. *Sheng Li Xue Bao* **47**, 597–600. (in Chinese)
4. Cooper NJ, Sutton AJ, Abrams KR, Wailoo A, Turner D and Nicholson KG (2003) Effectiveness of neuraminidase inhibitors in treatment and prevention of influenza A and B: systematic review and meta-analyses of randomised controlled trials. *BMJ* **326**, 1235.
5. Crain SM and Shen KF (2004) Neuraminidase inhibitor, oseltamivir blocks GM1 ganglioside-regulated excitatory opioid receptor-mediated hyperalgesia, enhances opioid analgesia and attenuates tolerance in mice. *Brain Res* **995**, 260–266.
6. Gendreau PL, Petitto JM, Gariepy JL and Lewis MH (1998) D2-like dopamine receptor mediation of social-emotional reactivity in a mouse model of anxiety: strain and experience effects. *Neuropsychopharmacology* **18**, 210–221.
7. Hama R (2005) Discussion of the causal relationship between oseltamivir phosphate (Tamiflu), and sudden death and death from abnormal behavior. 37th Annual Meeting of the Japanese Society for Pediatric Infectious Diseases. November 2005 (abstract).
8. Hama R (2006) Tamiflu causes abnormal behaviors at noon (after taking first time) of the first day. Part 1. *The Informed Prescriber* **21**, 110–116. (in Japanese)
9. Hama R (2007) Oseltamivir's adverse reactions: fifty sudden deaths may be related to central suppression. *BMJ* **335**, 59.
10. Hui KS and Roberts MB (1975) An improved implantation pellet for rapid induction of morphine dependence in mice. *J Pharmacol* **27**, 569–573.
11. Izumi Y, Tokuda K, O'dell KA, Zorumski CF and Narahashi T (2007) Neuroexcitatory actions of Tamiflu and its carboxylate metabolite. *Neurosci Lett* **426**, 54–58.
12. Japan issues Tamiflu warning after child deaths. *Times* March 21, 2007. http://www.timesonline.co.uk/tol/news/world/asia/article1549260.ece.
13. Jefferson T, Demicheli V, Rivetti D, Jones M, Di Pietrantonj C and Rivetti A (2006) Antivirals for influenza in healthy adults: systematic review. *Lancet* **367**, 303–313.
14. Li CY, Yu Q, Ye ZQ, Sun Y, He Q, Li XM, Zhang W, Luo J, Gu X, Zheng X and Wei L (2007) A nonsynonymous SNP in human cytosolic sialidase in a small Asian population results in reduced enzyme activity: potential link with severe adverse reactions to oseltamivir. *Cell Res* **17**, 357–362.
15. Masuda Y (2007) Sialic acid-rich glycolipid of schizophrenia sera. *Akita J Med* **34**, 123–127.
16. Masuda Y, Sugawara J, Ohnuma S and Sugiyama T (2002) Humoral GalNAcα1–3GalNAc-lipid reactivity of humans in hypomanic state. *Tohoku J Exp Med* **197**, 115–118.
17. Masuda Y, Suzuki M, Takemura T, Sugawara J, Guo N, Liu Y, Kawarada Y, Shimizu T and Sugiyama T (2003) Pharmacological mechanism in slip-down behavior of mice. *Tohoku J Exp Med* **201**, 23–27.
18. Maxwell SR (2007) Tamiflu and neuropsychiatric disturbance in adolescents. *BMJ* **334**, 1232–1233.
19. National Institute for Clinical Excellence. *Amantadine, oseltamivir and zanamivir for the treatment of influenza (review of existing guidance No. 58)*. October 2007. http://guidance.nice.org.uk/page.aspx?o=456310.
20. Okumura A, Kubota T, Kato T and Morishima T (2006) Oseltamivir and delirious behavior in children with influenza. *Pediatr Infect Dis J* **25**, 572.
21. Radad K, Gille G, Moldzio R, Saito H and Rausch WD (2004) Ginsenosides Rb1 and Rg1 effects on mesencephalic dopaminergic cells stressed with glutamate. *Brain Res* **1021**, 41–53.
22. Rodriguez JA, Piddini E, Hasegawa T, Miyagi T and Dotti CG (2001) Plasma membrane ganglioside sialidase regulates axonal growth and regeneration in hippocampal neurons in culture. *J Neurosci* **21**, 8387–8395.
23. Satoh K, Nonaka R, Ogata A, Nakae D and Uehara S (2007) Effects of oseltamivir phosphate (Tamiflu) and its metabolite (GS4071) on monoamine neurotransmission in the rat brain. *Biol Pharm Bull* **30**, 1816–1818.
24. Schauer R (2000) Achievements and challenges of sialic acid research. *Glycoconj J* **17**, 485–499.
25. Seyrantepe V, Poupetova H, Froissart R, Zabot MT, Maire I and Pshezhetsky AV (2003) Molecular pathology of NEU1 gene in sialidosis. *Hum Mutat* **22**, 343–352.
26. Traving C and Schauer R (1998) Structure, function and metabolism of sialic acids. *Cell Mol Life Sci* **54**, 1330–1349.

0090-9556/09/3702-264–267$20.00
DRUG METABOLISM AND DISPOSITION
Copyright © 2009 by The American Society for Pharmacology and Experimental Therapeutics
DMD 37:264–267, 2009

Vol. 37, No. 2
24943/3433052
Printed in U.S.A.

Short Communication

Activation of the Antiviral Prodrug Oseltamivir Is Impaired by Two Newly Identified Carboxylesterase 1 Variants

Received September 28, 2008; accepted November 18, 2008

ABSTRACT:

Oseltamivir phosphate is an ethyl ester prodrug widely used in the treatment and prevention of both Influenzavirus A and B infections. The conversion of oseltamivir to its active metabolite oseltamivir carboxylate is dependent on ester hydrolysis mediated by carboxylesterase 1 (CES1). We recently identified two functional CES1 variants p.Gly143Glu and p.Asp260fs in a research subject who displayed significant impairment in his ability to metabolize the selective CES1 substrate, methylphenidate. In vitro functional studies demonstrated that the presence of either of the two mutations can result in severe reductions in the catalytic efficiency of CES1 toward methylphenidate, which is required for hydrolysis and pharmacological deactivation. The aim of the present study was to investigate the function of these mutations on activating (hydrolyzing) oseltamivir to oseltamivir carboxylate using the cell lines expressing wild type (WT) and each mutant CES1. In vitro incubation studies demonstrated that the S9 fractions prepared from the cells transfected with WT CES1 and human liver tissues rapidly convert oseltamivir to oseltamivir carboxylate. However, the catalytic activity of the mutant hydrolases was dramatically hindered. The V_{max} value of p.Gly143Glu was approximately 25% of that of WT enzyme, whereas the catalytic activity of p.Asp260fs was negligible. These results suggest that the therapeutic efficacy of oseltamivir could be compromised in treated patients expressing either functional CES1 mutation. Furthermore, the potential for increased adverse effects or toxicity as a result of exposure to high concentrations of the nonhydrolyzed prodrug should be considered.

Oseltamivir phosphate (Tamiflu; Roche, Nutley, NJ) is widely used in the treatment and prophylaxis of both Influenzavirus A and B infections. In addition, oseltamivir may be effective in preventing or treating avian influenza or so-called "bird flu." Oseltamivir is an ester prodrug and, in general, it is readily converted to its active form oseltamivir carboxylate mediated by hepatic carboxylesterase 1 (CES1) (Fig. 1) (Shi et al., 2006). The active metabolite exerts its antiviral effects via the selective inhibition of neuraminidase.

Carboxylesterases are members of the $\alpha\beta$ hydrolase -fold family and expressed in many tissues, especially in the liver, small intestine, and lung (Satoh and Hosokawa, 2006; Ross and Crow, 2007). The major human carboxylesterases include CES1 (UniProtKB/Swiss-Prot P23141) and carboxylesterase 2 (CES2) (UniProtKB/Swiss-Prot O00748). CES1 and CES2 are largely distinguished from one another by their substrate specificity and tissue distribution (Imai et al., 2006; Satoh and Hosokawa, 2006). CES1 more readily catalyzes substrates with a relatively large acyl group and small alcohol group such as methylphenidate, temocapril, and oseltamivir (Sun et al., 2004; Imai et al., 2005; Shi et al., 2006). In contrast, CES2 preferentially hydrolyzes compounds bearing a small acyl moiety and bulky alcohol group, which includes agents such as cocaine and irinotecan. CES1 predominates in the human liver, whereas CES2 is the major carboxylesterase expressed in the intestine (Imai et al., 2006). Hepatic CES1 is the major esterase governing the metabolism of numerous and structurally diverse therapeutic agents formulated as carboxylic acid esters, carbamates, thioesters, and amide compounds including those prodrugs formulated as esters. In addition, a number of endogenous substrates are recognized.

In a recent study, we identified two CES1 mutations, p.Gly143Glu and p.Asp260fs (Zhu et al., 2008), in a subject who displayed profound alteration of the pharmacokinetics of racemic (*dl*)-methylphenidate (Ritalin; Novartis Pharmaceuticals, Summit, NJ), a selective CES1 substrate, during a single-dose pharmacokinetic study (Patrick et al., 2007). The minor allele frequency of p.Gly143Glu was estimated to be 3.7, 4.3, 2.0, and 0% in white, black, Hispanic, and Asian populations, respectively, by a genotyping study that contains a total of 925 subjects with varied racial and ethnic backgrounds. It was concluded that the p.Asp260fs variant was extremely rare because none of the 925 screened subjects carried this mutation. The functional consequences of both mutations were investigated using cell lines stably expressing each individual mutant. The in vitro incubation study demonstrated that the catalytic function of both p.Gly143Glu and p.Asp260fs is impaired to such a significant degree that CES1-mediated methylphenidate hydrolysis was essentially nil using these two CES1 mutants, whereas wild-type (WT) CES1 readily cleaved the ester (Zhu et al., 2008).

Even though the two newly discovered *CES1* mutations were determined to be dysfunctional enzymes in terms of hydrolyzing methylphenidate to its inactive metabolite ritalinic acid, the influence of these *CES1* variants on prodrug activation has not been examined to date. Oseltamivir (a drug in wide therapeutic use) has recently been shown to be a selective

Article, publication date, and citation information can be found at http://dmd.aspetjournals.org.
doi:10.1124/dmd.108.024943.

ABBREVIATIONS: CES1, carboxylesterase 1; CES2, carboxylesterase 2; WT, wild type; PNPA, *p*-nitrophenyl acetate; PNP, *p*-nitrophenol; HPLC, high-performance liquid chromatography.

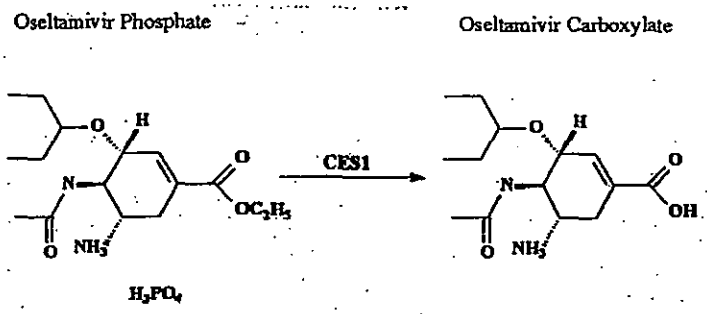

FIG. 1. CES1-mediated activation of oseltamivir phosphate.

substrate of CES1 (Shi et al., 2006), making it an excellent candidate compound to assess the effect(s) of the identified *CES1* mutations on prodrug activation. In addition, accumulating evidence has indicated that the biotransformation of oseltamivir phosphate to the primary active form oseltamivir carboxylate is not only related to its antiviral efficacy but also associated with potential toxicity (http://www.fda.gov/cder/foi/nda/2000/21-246_Tamiflu_Pharmr.pdf).

In the present study, we investigated the influence of the two newly identified CES1 variants on the metabolism (i.e., activation) of the prodrug oseltamivir phosphate. The results suggested that genetic variants of *CES1* that result in dysfunctional enzyme activity could likewise play an important role in both therapeutic efficacy as well as tolerability or toxicity during oseltamivir therapy.

Materials and Methods

Materials. Oseltamivir phosphate and its active metabolite oseltamivir carboxylate were obtained from Toronto Research Chemicals Inc. (North York, ON. Canada). *p*-nitrophenyl acetate (PNPA) and *p*-nitrophenol (PNP) were purchased from Sigma-Aldrich (St. Louis, MO). All other chemicals and reagents were of the highest analytical grade and were commercially available.

Enzymatic Study. The establishment of Flp-In-293 cells (Invitrogen, Carlsbad, CA) stably expressing WT and p.Gly143Glu and p.Asp260fs CES1 has been described previously (Zhu et al., 2008). The transfected cells were cultured in Dulbecco's modified Eagle's medium containing 10% fetal bovine serum and 100 μg/ml hygromycin B. After reaching approximately 95% confluence, cells were then washed and harvested in reaction buffer (phosphate-buffered saline containing 10 mM HEPES, pH 7.4). Afterward, cells were sonicated and then centrifuged at 9000*g* for 30 min at 4°C. The supernatant (S9 fraction) was collected and stored at −70°C until use. The liver tissues were obtained from a healthy liver donor and determined to express neither p.Gly143Glu nor the p.Asp260fs mutation and served as a native CES1 control. The liver samples (~300 mg) were homogenized, and the S9 fraction was obtained after centrifugation at 9000*g* for 30 min at 4°C. The protein concentrations were determined using a Pierce BCA assay kit (Pierce, Rockford, IL).

The oseltamivir hydrolysis study was carried out in 1.5-ml tubes at a total volume of 100 μl. Before incubations, oseltamivir phosphate solutions were freshly prepared in 50 μl of reaction buffer. The reaction was initiated by mixing oseltamivir phosphate with 50 μl of S9 fractions. The final oseltamivir phosphate concentrations ranged from 10 to 5000 μM. Our preliminary study indicated that the formation of oseltamivir carboxylate was linear with a series of S9 protein concentrations (0.05–0.5 mg/ml) and incubation times (5–15 min) that we tested. In the present study, the enzymatic reactions were performed with the final S9 protein concentration standardized at 0.1 mg/ml and an incubation period of 10 min at 37°C. After incubation, the reaction was terminated by adding 500 μl of methanol containing 40 μM ritalinic acid as the internal standard. The mixture was centrifuged at 16,000*g* for 5 min to precipitate protein, and the supernatants were then analyzed using an established high-performance liquid chromatography (HPLC) assay. Enzyme kinetic data of oseltamivir hydrolysis were fit to the Michaelis-Menten equation, and kinetic parameters K_m and V_{max} were calculated using nonlinear regression analysis with GraphPad Prism software (GraphPad Software Inc., San Diego, CA). In addition, PNPA, a widely used esterase substrate (including CES1), was included in the study as a positive control using a method described previously (Zhu et al., 2008).

HPLC Analysis. An HPLC method was used to measure oseltamivir carboxylate formation as a consequence of oseltamivir phosphate hydrolysis. The HPLC system consisted of an Agilent 1100 HPLC system (Agilent Technologies, Santa Clara, CA) equipped with a diode-array detector with the wavelength set at 220 nm. The mobile phase was a mixture of methanol and 20 mM KH_2PO_4 (pH2.5). A gradient elution was applied for the separation with the time program set as follows: from 0 to 4 min, methanol was 44%, and increased to 50% from 4 to 14 min, then maintained at 50% until 16 min, where methanol was returned to the initial condition (44%). Ritalinic acid, oseltamivir carboxylate, and oseltamivir were eluted at 5.1, 6.0, and 15.7 min, respectively, with the flow rate set at 1 ml/min. In Fig. 2, a typical chromatogram is represented of 100 μM of oseltamivir hydrolyzed by WT *CES1* S9 fractions after incubation. The intraday and interday relative standard deviations were determined to be less than 10%. The lower limit of quantification of oseltamivir carboxylate was 0.25 μM.

Results

PNPA is a sensitive and established model substrate of CES1 as well as other human esterases. The PNPA hydrolysis assay demonstrated that WT CES1 prepared from the cells transfected with WT *CES1* gene rapidly hydrolyzed PNPA to PNP with a catalytic efficiency comparable with that of normal human liver tissues (Fig. 3). Consistent with our previous observations, the enzymatic activity of both p.Gly143Glu and p.Asp260fs toward PNPA was dramatically reduced relative to WT enzyme (Zhu et al., 2008).

The oseltamivir phosphate incubation study demonstrated that the S9 preparations of both WT CES1-transfected cells and human liver tissues efficiently convert oseltamivir to its active antiviral component, oseltamivir carboxylate, suggesting that oseltamivir serves as an excellent substrate of CES1 (Fig. 3). The V_{max} and K_m values were determined to be 145 ± 5 nmol/min/mg protein and 1.38 ± 0.13 mM, respectively, under our experimental conditions (Fig. 4). The CES1 variants p.Gly143Glu and p.Asp260fs displayed poor catalytic activity toward oseltamivir hydrolysis (Figs. 3 and 4). The V_{max} value of p.Gly143Glu was found to be 37 ± 1 nmol/min/mg protein, which is approximately 25% of that of WT CES1. The K_m value of p.Gly143Glu was estimated to be 2.15 ± 0.18 mM. In addition, p.Asp260fs failed to produce any detectable hydrolysis of oseltamivir as measured by the formation of oseltamivir carboxylate (Fig. 3). The human liver S9 fractions prepared from a healthy donor specimen produced similar catalytic activity toward both PNPA and oseltamivir phosphate, which was in excellent agreement with that of our W *CES1*-transfected cells (Fig. 3).

Discussion

CES1 is the predominant hydrolase in the liver and plays an important role in the biotransformation of drugs and prodrugs that contains ester bonds. CES1 genetic variants and their potential for having therapeutic implications have been increasingly reported recently. Our previous study identified two nonsynonymous coding region variants, p.Gly143Glu and p.Asp260fs. In vitro functional studies have shown that the catalytic function mediating the typically efficient and rapid hydrolysis of methylphenidate was clearly disrupted in both the p.Gly143Glu variant and the p.Asp260fs mutation. The potential for clinically significant outcomes in the presence of these two mutations was investigated in the original subject found to carry both CES1 variants. That subject displayed an extremely abnormal pharmacokinetic profile after the administration of methylphenidate, displaying vastly higher overall blood concentrations of methylphenidate and an unprecedented distortion in the disposition of the respective isomers of the drug (Patrick et al., 2007; Zhu et al., 2008).

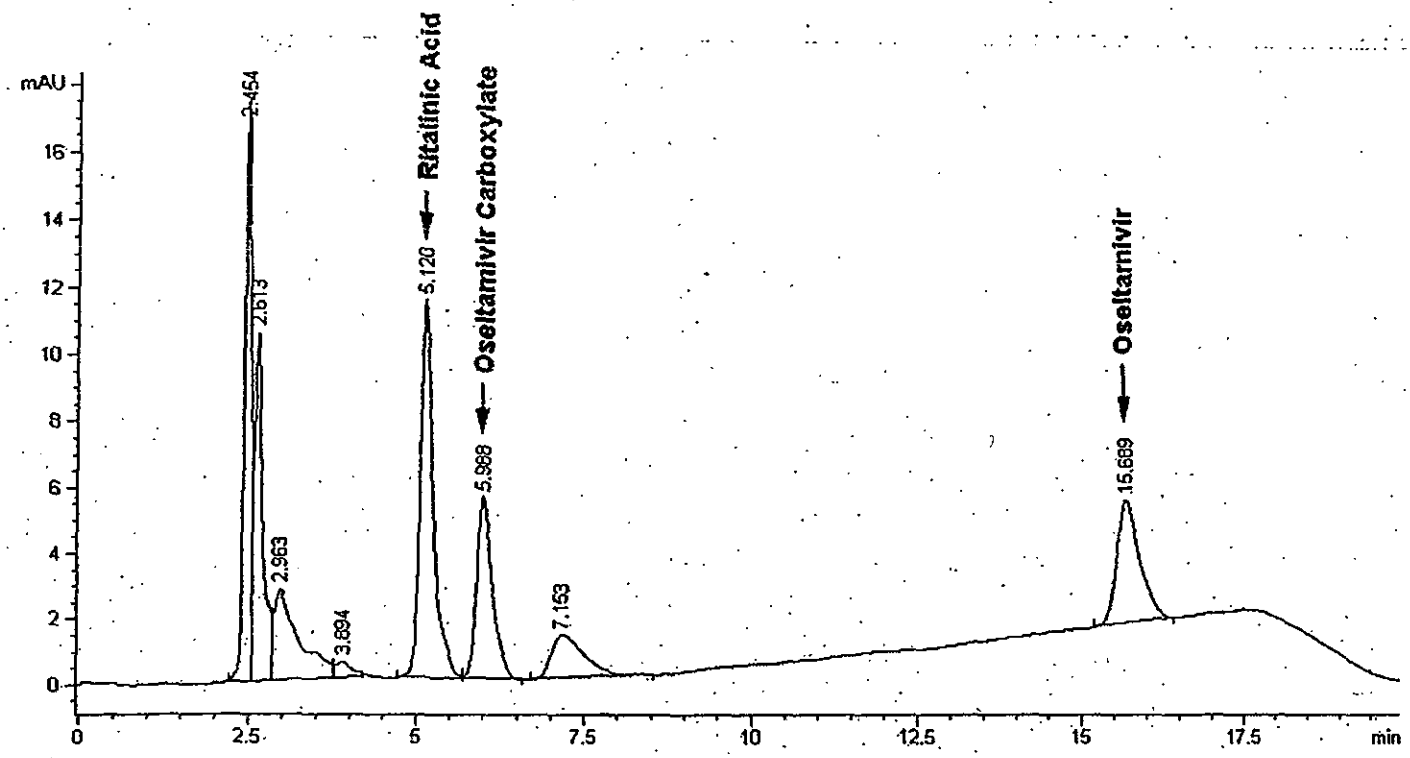

FIG. 2. Representative chromatograph of oseltamivir carboxylate. Oseltamivir carboxylate was analyzed by the HPLC assay after incubation of oseltamivir phosphate (100 μM) and WT CES1 S9 fractions at 37°C for 10 min.

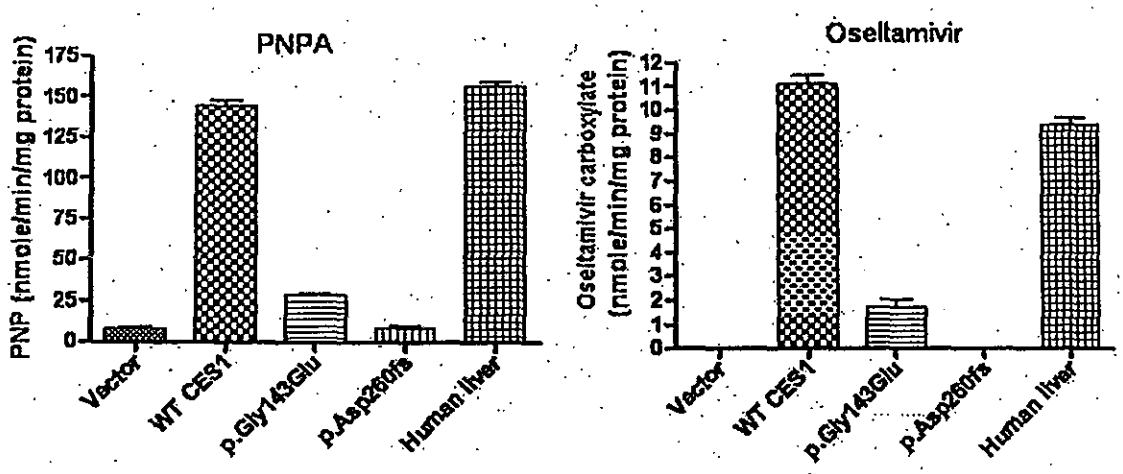

FIG. 3. Hydrolysis of PNPA and oseltamivir by human liver microsomal, WT CES1, and its mutants p.Gly143Glu and p.Asp260fs. The hydrolytic products of PNPA and oseltamivir were determined after incubating the substrates with the enzymes at 37°C for 10 min. Data were expressed as the mean ± S.D. (n = 4).

In addition, the subject experienced significantly higher cardiovascular vital signs relative to other 19 study subjects serving as a pharmacodynamic correlate to the pharmacokinetic observations (Zhu et al., 2008).

Because the activation of many ester prodrugs depends to a great degree upon functional CES1 enzyme to produce the therapeutic moiety, dysfunctional CES1 variants could hinder prodrug activation and lead to the alteration of therapeutic effects and accumulation of the parent prodrug with continued dosing. Such an outcome could lead to therapeutic failure and, depending on the compound administered, unanticipated adverse effects or toxicities. As a prodrug, oseltamivir does not exhibit activity toward the influenza virus unless it is converted to its active metabolite oseltamivir carboxylate by CES1 (Fig. 1). In the present study, the catalytic activity of p.Gly143Glu and p.Asp260fs toward oseltamivir hydrolysis (i.e., activation) was investigated using transfected cell lines stably expressing WT and individual mutant CES1 enzyme. The data indicated that the enzymatic activity of p.Gly143Glu is substantially decreased with a V_{max} value approximately one fourth that of WT CES1, whereas p.Asp260fs failed to show any measurable hydrolytic activity toward oseltamivir. Acknowledging the limitations of in vitro methodologies, this fundamental alteration in the catalytic activity of CES1 strongly suggests that the activation of oseltamivir would be compromised in patients who express such *CES1* variants. In addition to these two mutations, several other natural nonconservative *CES1* variants were recently determined to also have functional significance (Shi et al., 2006; Tang et al., 2006). Furthermore, beyond the coding area mutations, a number of functional variants have been reported in the transcriptional regulation region of *CES1* gene (Geshi et al., 2005; Hosokawa et al., 2008; Yoshimura et al., 2008). Among those, a single nucleotide

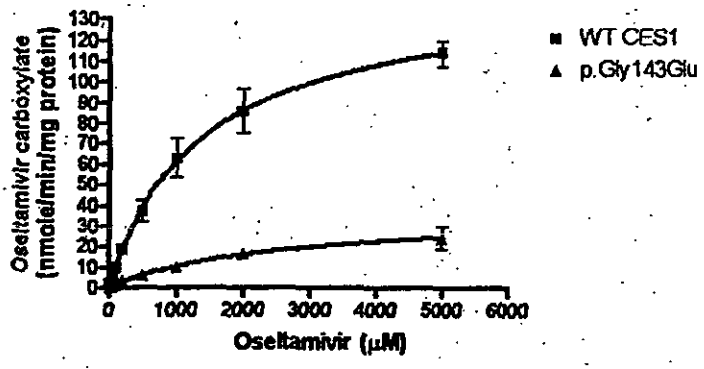

FIG. 4. Enzymatic kinetics study of oseltamivir hydrolysis catalyzed by WT CES1 and its variant p.Gly143Glu. The hydrolysis of oseltamivir (10–5000 μM) was determined after incubation with the cell S9 fractions at 37°C for 10 min. The V_{max} and K_m values were calculated using nonlinear regression analysis with GraphPad Prism software. Data present means ± S.D. for four independent experiments.

polymorphism, −816A/C of the *CES1A2* gene was found to be associated with an improved therapeutic response to an angiotensin-converting enzyme inhibitor imidapril, which is a prodrug and selectively activated by CES1 (Geshi et al., 2005).

It was noted that the observed V_{max} value of WT CES1 is consistent with that reported by Shi et al. (2006), whereas the K_m value is seven times higher. We suspect this difference is more likely than not the result of different experimental conditions used in these two independent studies. For example, the reaction buffer used in the present study was phosphate-buffered saline containing 10 mM HEPES (pH 7.4), whereas a Tris buffer was used in the study by Shi et al. (2006). Indeed, a recent in vitro study addressing this very issue indicates that different enzymatic activity of CES could be observed when different assay buffers were used (Williams et al., 2008). Finally, the S9 fractions used in the present study were prepared from a stable CES1 cell line rather than a transient expression assay.

Functional CES1 is not only critical for the conversion of oseltamivir to its active metabolite to achieve a favorable therapeutic response, but it is also related to the toxicity during oseltamivir therapy. Converging evidence suggests that CES1 function in juvenile animals remain at a significantly lower level than that of adult animals (Kadner et al., 1992; Morgan et al., 1994; Moser et al., 1998; Karanth and Pope, 2000; Padilla et al., 2004; Anand et al., 2006). Animal studies demonstrated that juvenile rats did not hydrolyze oseltamivir efficiently, and they are more susceptible than adults to oseltamivir toxicity (http://www.fda.gov/cder/foi/nda/2000/21-246_Tamiflu_Pharmr.pdf). The present study suggests that, in addition to age, genetic variation is potentially an important factor influencing the enzymatic function of CES1 and could play a role in the therapeutic outcome and toxicity of pharmacotherapy with oseltamivir as well as other known CES1 substrates. Our previously published data with the psychostimulant methylphenidate indicate that the effects of *CES1* variants on drug disposition are already advanced beyond the realm of speculation.

In summary, two newly identified *CES1* mutations p.Gly143Glu and p.Asp260fs were determined to be dysfunctional enzymes with respect to the activation of the prodrug oseltamivir. Impaired enzymatic function could have significant implications with regard to both the therapeutic efficacy and tolerability of oseltamivir. It should be noted that the extremely low prevalence of p.Asp260fs mutation relegates its clinical significance to being very minor even though it results in a nonfunctional enzyme. However, p.Gly143Glu is a common variant in all populations assessed thus far, with the exception of Asians. A clinical study, particularly one assessing patients who have been genotyped and found to be heterozygously expressing p.Gly143Glu, is warranted to elucidate the influence of the p.Gly143Glu mutation on the pharmacological disposition and potential toxicities of oseltamivir.

Department of Pharmaceutical and Biomedical Sciences,
Laboratory of Drug Disposition and Pharmacogenetics,
Charles P. Darby Children's Research Institute,
Medical University of South Carolina,
Charleston, South Carolina

HAO-JIE ZHU
JOHN S. MARKOWITZ

References

Anand SS, Kim KB, Padilla S, Muralidhara S, Kim HJ, Fisher JW, and Bruckner JV (2006) Ontogeny of hepatic and plasma metabolism of deltamethrin in vitro: role in age-dependent acute neurotoxicity. *Drug Metab Dispos* 34:389–397.

Geshi E, Kimura T, Yoshimura M, Suzuki H, Koba S, Sakai T, Saito T, Koga A, Muramatsu M, and Katagiri T (2005) A single nucleotide polymorphism in the carboxylesterase gene is associated with the responsiveness to imidapril medication and the promoter activity. *Hypertens Res* 28:719–725.

Hosokawa M, Furihata T, Yaginuma Y, Yamamoto N, Watanabe N, Tsukada E, Ohhata Y, Kobayashi K, Satoh T, and Chiba K (2008) Structural organization and characterization of the regulatory element of the human carboxylesterase (CES1A1 and CES1A2) genes. *Drug Metab Pharmacokinet* 23:73–84.

Imai T, Imoto M, Sakamoto H, and Hashimoto M (2005) Identification of esterases expressed in Caco-2 cells and effects of their hydrolyzing activity in predicting human intestinal absorption. *Drug Metab Dispos* 33:1185–1190.

Imai T, Taketani M, Shii M, Hosokawa M, and Chiba K (2006) Substrate specificity of carboxylesterase isozymes and their contribution to hydrolase activity in human liver and small intestine. *Drug Metab Dispos* 34:1734–1741.

Kadner SS, Katz J, and Finlay TH (1992) Esterase-1: developmental expression in the mouse and distribution of related proteins in other species. *Arch Biochem Biophys* 296:435–441.

Karanth S and Pope C (2000) Carboxylesterase and A-esterase activities during maturation and aging: relationship to the toxicity of chlorpyrifos and parathion in rats. *Toxicol Sci* 58:282–289.

Morgan EW, Yan B, Greenway D, and Parkinson A (1994) Regulation of two rat liver microsomal carboxylesterase isozymes: species differences, tissue distribution, and the effects of age, sex, and xenobiotic treatment of rats. *Arch Biochem Biophys* 315:513–526.

Moser VC, Chanda SM, Mortensen SR, and Padilla S (1998) Age- and gender-related differences in sensitivity to chlorpyrifos in the rat reflect developmental profiles of esterase activities. *Toxicol Sci* 46:211–222.

Padilla S, Sung HJ, and Moser VC (2004) Further assessment of an in vitro screen that may help identify organophosphorus pesticides that are more acutely toxic to the young. *J Toxicol Environ Health A* 67:1477–1489.

Patrick KS, Straughn AB, Minhinnett RR, Yeatts SD, Herrin AE, DeVane CL, Malcolm R, Janis GC, and Markowitz JS (2007) Influence of ethanol and gender on methylphenidate pharmacokinetics and pharmacodynamics. *Clin Pharmacol Ther* 81:346–353.

Ross MK and Crow JA (2007) Human carboxylesterases and their role in xenobiotic and endobiotic metabolism. *J Biochem Mol Toxicol* 21:187–196.

Satoh T and Hosokawa M (2006) Structure, function and regulation of carboxylesterases. *Chem Biol Interact* 162:195–211.

Shi D, Yang J, Yang D, LeCluyse EL, Black C, You L, Akhlaghi F, and Yan B (2006) Anti-influenza prodrug oseltamivir is activated by carboxylesterase human carboxylesterase 1 and the activation is inhibited by antiplatelet agent clopidogrel. *J Pharmacol Exp Ti* 319:1477–1484.

Sun Z, Murry DJ, Sanghani SP, Davis WI, Kedishvili NY, Zou Q, Hurley TD, and Bosron WF (2004) Methylphenidate is stereoselectively hydrolyzed by human carboxylesterase CES1A1. *J Pharmacol Exp Ther* 310:469–476.

Tang M, Mukundan M, Yang J, Charpentier N, LeCluyse EL, Black C, Yang D, Shi D, and Yan B (2006) Antiplatelet agents aspirin and clopidogrel are hydrolyzed by distinct carboxylesterases, and clopidogrel is transesterificated in the presence of ethyl alcohol. *J Pharmacol Exp Ther* 319:1467–1476.

Williams ET, Ehsani ME, Wang X, Wang H, Qian YW, Wrighton SA, and Perkins EJ (2008) Effect of buffer components and carrier solvents on in vitro activity of recombinant human carboxylesterases. *J Pharmacol Toxicol Methods* 57:138–144.

Yoshimura M, Kimura T, Ishii M, Ishii K, Matsuura T, Geshi E, Hosokawa M, and Muramatsu M (2008) Functional polymorphisms in carboxylesterase1A2 (CES1A2) gene involves specific protein 1 (Sp1) binding sites. *Biochem Biophys Res Commun* 369:939–942.

Zhu HJ, Patrick KS, Yuan HJ, Wang JS, Donovan JL, DeVane CL, Malcolm R, Johnson JA, Youngblood GL, Sweet DH, et al. (2008) Two CES1 gene mutations lead to dysfunctional carboxylesterase 1 activity in man: clinical significance and molecular basis. *Am J Hum Genet* 82:1241–1248.

Address correspondence to: Dr. Hao-Jie Zhu, Charles P. Darby Children's Research Institute, Room 405B, Medical University of South Carolina, 173 Ashley Avenue, Charleston, SC 29425. E-mail: zhuh@musc.edu

0090-9556/09/3702-315–321$20.00
DRUG METABOLISM AND DISPOSITION
Copyright © 2009 by The American Society for Pharmacology and Experimental Therapeutics
DMD 37:315–321, 2009

Vol. 37, No. 2
24018/3434124
Printed in U.S.A.

Limited Brain Distribution of [3*R*,4*R*,5*S*]-4-Acetamido-5-amino-3-(1-ethylpropoxy)-1-cyclohexene-1-carboxylate Phosphate (Ro 64-0802), a Pharmacologically Active Form of Oseltamivir, by Active Efflux across the Blood-Brain Barrier Mediated by Organic Anion Transporter 3 (Oat3/*Slc22a8*) and Multidrug Resistance-Associated Protein 4 (Mrp4/*Abcc4*)

Atsushi Ose, Mototsugu Ito, Hiroyuki Kusuhara, Kenzo Yamatsugu, Motomu Kanai, Masakatsu Shibasaki, Masakiyo Hosokawa, John D. Schuetz, and Yuichi Sugiyama

Graduate School of Pharmaceutical Sciences, the University of Tokyo, Bunkyo-ku, Tokyo, Japan (A.O., M.I., H.K., K.Y., M.K., M.S., Y.S.); Chiba Institute of Science, Choshi-city, Chiba, Japan (M.H.); and Department of Pharmaceutical Sciences, St. Jude Children's Research Hospital, Memphis, Tennessee (J.D.S.)

Received August 18, 2008; accepted November 20, 2008

ABSTRACT:

[3*R*,4*R*,5*S*]-4-Acetamido-5-amino-3-(1-ethylpropoxy)-1-cyclohexene-1-carboxylate phosphate (Ro 64-0802) is a pharmacologically active form of the anti-influenza virus drug oseltamivir. Abnormal behavior is a suspected adverse effect of oseltamivir on the central nervous system. This study focused on the transport mechanisms of Ro 64-0802 across the blood-brain barrier (BBB). Ro 64-0802 was found to be a substrate of organic anion transporter 3 (OAT3/*SLC22A8*) and multidrug resistance-associated protein 4 (MRP4/*ABCC4*). Human embryonic kidney 293 cells expressing OAT3 exhibited a greater intracellular accumulation of Ro 64-0802 than mock-transfected cells (15 versus 1.2 μl/mg protein/10 min, respectively). The efflux of Ro 64-0802 was 3-fold greater when MRP4 was expressed in MDCKII cells and was significantly inhibited by indomethacin. After its microinjection into the cerebrum, the amount of Ro 64-0802 in brain was significantly greater in both *Oat3*$^{-/-}$ mice and *Mrp4*$^{-/-}$ mice compared with the corresponding wild-type mice (0.36 versus 0.080 and 0.32 versus 0.060 nmol at 120 min after injection, respectively). The brain/plasma concentration ratio ($K_{p,brain}$) of Ro 64-0802, determined in wild-type mice after subcutaneous continuous infusion for 24 h, was close to the capillary volume (approximately 10 μl/g brain). Although the $K_{p,brain}$ of Ro 64-0802 was unchanged in *Oat3*$^{-/-}$ mice, it was significantly greater in *Mrp4*$^{-/-}$ mice (41 μl/g of brain). These results suggest that Ro 64-0802 can cross the BBB from the blood, but its brain distribution is limited by its active efflux by Mrp4 and Oat3 across the BBB. The transporter responsible for the brain uptake of Ro 64-0802 remains unknown, but Oat3 is a candidate transporter.

Oseltamivir is an ester-type prodrug of Ro 64-0802, a potent and selective inhibitor of viral neuraminidase, a key enzyme involved in the release of influenza virus from host cells. Oseltamivir is used for the treatment and prophylaxis of infectious diseases caused by both Influenzavirus A and Influenzavirus B (Bardsley-Elliot and Noble, 1999). In recent studies, abnormal behavior, such as jumping and falling from balconies, has been reported in teenagers or younger people who are taking oseltamivir (http://www.fda.gov/cder/drug/infopage/tamiflu/QA20051117.htm; Fuyuno, 2007). In response to these reports, the Ministry of Health, Labor and Welfare has issued a warning regarding the use of oseltamivir as a medication for teenagers or younger people and has prohibited the prescribing of oseltamivir for them in Japan.

The pharmacological actions of oseltamivir on the central nervous system have been reported in several animal studies (Izumi et al., 2007; Satoh et al., 2007; Usami et al., 2008; Yoshino et al., 2008), although the association between such pharmacological actions and abnormal behavior remains an open question. The systemic administration of oseltamivir increases dopamine levels in the rat medial prefrontal cortex (Yoshino et al., 2008), and oseltamivir and Ro

This work supported in part by a grant-in-aid for Scientific Research (A) [Grant 20249008] and Scientific Research (B) [Grant 20390046] from the Ministry of Education, Culture, Sports, Science and Technology.

Article, publication date, and citation information can be found at http://dmd.aspetjournals.org.

doi:10.1124/dmd.108.024018.

ABBREVIATIONS: Ro 64-0802, [3*R*,4*R*,5*S*]-4-acetamido-5-amino-3-(1-ethylpropoxy)-1-cyclohexene-1-carboxylate phosphate; BBB, blood-brain barrier; CES1A1, carboxylesterase 1A1; P-gp, P-glycoprotein; Oat/OAT, organic anion transporter; Mrp/MRP, multidrug resistance-associated protein; HEK, human embryonic kidney; MDCK, Madin-Darby canine kidney; LC, liquid chromatography; MS, mass spectrometry; GFP, green fluorescent protein; ANOVA, analysis of variance; PCR, polymerase chain reaction; Mdr, multidrug resistance; Bcrp, breast cancer resistance protein; Oatp, organic anion transporter peptide.

64-0802 enhance spike synchronization between hippocampal CA3 pyramidal cells and evoked synchronized population bursts, which recruit virtually all of the neurons in the network (Usami et al., 2008). It has also been demonstrated that oseltamivir and Ro 64-0802 affect neuronal excitability in rat hippocampal slices and that Ro 64-0802 is 30 times more potent than oseltamivir (Izumi et al., 2007).

Whether oseltamivir and Ro 64-0802 cross the blood-brain barrier (BBB) is an important issue, considering their pharmacological actions on the central nervous system. In clinical studies, both oseltamivir and Ro 64-0802 were detected in the plasma after oral administration of oseltamivir. Oseltamivir is converted to Ro 64-0802 by carboxylesterase 1A1 (CES1A1) in the liver (Shi et al., 2006). Most of the administered dose is recovered in the urine as Ro 64-0802 by glomerular filtration and tubular secretion by organic anion transporters in the kidney (He et al., 1999). The penetration of drugs to the brain from the circulating blood is limited by the BBB, which is formed by endothelial cells connected tightly to adjacent cells. It has been shown that oseltamivir can cross the BBB, but P-glycoprotein (P-gp) limits its brain penetration at the BBB (Morimoto et al., 2008; Ose et al., 2008). In contrast, Ro 64-0802 exhibits only a limited distribution in the brain because it is close to the brain capillary volume. Therefore, the permeability of Ro 64-0802 across the BBB has been considered to be quite low because of its hydrophilic nature and anionic charge at neutral pH.

In this study, we hypothesized that the low distribution of Ro 64-0802 in the brain is attributable to active efflux at the BBB. We focused on two organic anion transporters—organic anion transporter 3 (OAT3/*SLC22A8*) and multidrug resistance-associated protein 4 (MRP4/*ABCC4*)—as the candidate transporters involved. Oat3 is expressed on the abluminal membrane of the brain capillary endothelial cells in rodents (Kikuchi et al., 2003; Mori et al., 2003; Roberts et al., 2008). Cumulative in vivo studies suggest that Oat3 plays a significant role in the uptake of hydrophilic organic anions into the endothelial cells, the first step in its overall elimination from the brain to the blood (Ohtsuki et al., 2002; Kikuchi et al., 2003, 2004; Mori et al., 2003, 2004). Ro 64-0802 has been identified as a substrate of OAT1/*SLC22A6* (Hill et al., 2002). Considering the overlapping substrate specificities of OAT1 and OAT3, it is possible that OAT3 accepts Ro 64-0802 as substrate. MRP4 is an ATP-binding cassette transporter localized in the luminal membrane of the brain capillary endothelial cells (Leggas et al., 2004). MRP4 accepts anionic drugs as substrates (Ci et al., 2007; Hasegawa et al., 2007; Imaoka et al., 2007) and mediates their unidirectional efflux into the circulating blood (Leggas et al., 2004). It has been demonstrated that the elimination of topotecan from the brain was delayed and that the concentration of topotecan in the cerebrospinal fluid was greatly enhanced in *Mrp4*$^{-/-}$ mice compared with the corresponding wild-type mice (Leggas et al., 2004). It has also been demonstrated that the brain/plasma concentration ratio of 9′-(2′-phosphonylmethoxyethyl)-adenine 3 h after intravenous administration was greater in *Mrp4*$^{-/-}$ mice than in wild-type mice (Belinsky et al., 2007).

In this study, in vivo experiments were undertaken using wild-type, *Oat3*$^{-/-}$, and *Mrp4*$^{-/-}$ mice to examine the involvement of Oat3 and Mrp4 in the uptake and efflux of Ro 64-0802 across the BBB.

Materials and Methods

Reagents. Oseltamivir phosphate and its active metabolite, Ro 64-0802 (purity >95%), were synthesized according to a previous report (Yamatsugu et al., 2007). All other chemicals used in the experiments were of analytical grade.

Animals. *Mrp4*$^{-/-}$ mice had been established previously (Leggas et al., 2004). *Oat3*$^{-/-}$ mice were obtained from Deltagen, Inc. (San Carlos, CA). Male C57BL/6J, *Mrp4*$^{-/-}$, and *Oat3*$^{-/-}$ mice were maintained by CLEA Japan, Inc. (Tokyo, Japan). All mice (10–18 weeks old) were maintained under standard conditions with a reverse dark-light cycle. Food and water were available ad libitum. All experiments using animals in this study were performed according to the guidelines provided by the Institutional Animal Care Committee (Graduate School of Pharmaceutical Sciences, University of Tokyo).

Uptake of Ro 64-0802 by Human OAT3-Expressing HEK293 Cells. An in vitro transport experiment was performed as described previously (Deguchi et al., 2004). After the cells had been washed twice and preincubated with Krebs-Henseleit buffer at 37°C for 15 min, drug uptake was initiated by the addition of Krebs-Henseleit buffer containing Ro 64-0802 (10 μM). The Krebs-Henseleit buffer consisted of 118 mM NaCl, 23.8 mM $NaHCO_3$, 4.8 mM KCl, 1.0 mM KH_2PO_4, 1.2 mM $MgSO_4$, 12.5 mM HEPES, 5.0 mM glucose, and 1.5 mM $CaCl_2$, adjusted to pH 7.4. Uptake was terminated at the designated times by the addition of ice-cold Krebs-Henseleit buffer after the removal of the incubation buffer. The cells were then washed twice with 1 ml of ice-cold Krebs-Henseleit buffer, solubilized in 500 μl of 1 mM Tris-HCl buffer (pH 7.4), and stored overnight at 4°C. After sonication, aliquots (250 μl) were subjected to liquid chromatography (LC)-mass spectrometry (MS) analysis. The remaining 20 μl of cell lysate was used to determine the protein concentration by the method of Lowry et al. (1951), with bovine serum albumin as the standard.

Construction of Human MRP4/CES1A1-Expressing MDCKII Cells. CES1A1 cDNA was subcloned into the pTARGET vector (Promega, Madison, WI) (Mori et al., 1999) and transfected into MDCKII cells with Lipofectamine 2000 reagent (Invitrogen, Carlsbad, CA), according to the manufacturer's protocol. The transfectants were selected by culturing them in the presence of neomycin (1600 μg/ml) (Invitrogen) and were maintained in Dulbecco's modified Eagle's medium (Invitrogen) supplemented with 10% fetal bovine serum, 1% antibiotic-antimycotic (Invitrogen), and neomycin (400 μg/ml) at 37°C with 5% CO_2 and 95% humidity. MDCKII cells with sufficient CES1A1 activity (CES1A1-MDCKII) were cloned and used as the hosts for infection with recombinant adenovirus carrying the human *MRP4* gene, which had been established previously (Ci et al., 2007; Hasegawa et al., 2007; Imaoka et al., 2007). CES1A1-MDCKII cells were infected with recombinant adenovirus containing human MRP4 transporter cDNA at a multiplicity of infection of 10 for 48 h to overexpress human MRP4 (MRP4/CES1A1-MDCKII). Green fluorescent protein (GFP) was used as the negative control (GFP/CES1A1-MDCKII).

The expression of MRP4 protein was confirmed by Western blotting. The cell lysates were loaded onto a SDS-polyacrylamide gel (7.5%) with a 3.75% stacking gel. *N*-Linked carbohydrate groups were cleaved from the MRP4 protein in the cell lysates with *N*-glycosidase F (PNGase F; New England Biolabs, Ipswich, MA). Digestion was performed according to the manufacturer's instructions, except that the samples were incubated for 30 min at 37°C in denaturing buffer rather than for the recommended 10 min at 100°C. To minimize protein degradation, protease inhibitors were included in all the steps. After incubation at 37°C for 30 min, the samples were separated by SDS-polyacrylamide gel electrophoresis (7.5%). The proteins were electroblotted on to a polyvinylidene difluoride membrane (Pall Corporation, East Hills, NY). The membrane was blocked with blocking buffer [Tris-buffered saline containing 0.05% Tween 20 (TTBS) and 3% skimmed milk] for 1 h at room temperature. After it had been washed with TTBS, the membrane was incubated overnight at 4°C with monoclonal anti-MRP4 M4I-10 antibody (1:1000 in blocking buffer; Abcam Inc., Cambridge, MA). The protein was detected by binding horseradish peroxidase-labeled anti-rat IgG antibody (1:5000 in blocking buffer; GE Healthcare, Little Chalfont, Buckinghamshire, UK). Immunoreactivity was detected with an ECL Plus Western Blotting Detection Kit (GE Healthcare).

***Efflux of Ro 64-0802 Formed Intracellularly from Oseltamivir in* MRP4/CES1A1-MDCKII and GFP/CES1A1-MDCKII Cells.** After the cells had been washed twice and preincubated with Krebs-Henseleit buffer at 37°C for 15 min, oseltamivir (10 μM) was added to the incubation buffer in the presence or absence of indomethacin (50 μM). At the designated times, the incubation buffer was collected. Ice-cold Krebs-Henseleit buffer was then added, and the cells were washed four times. After the cells had been collected, they were frozen in liquid nitrogen and stored at −80°C until use. The efflux

clearance of Ro 64-0802 from the transfectants was determined using the integration plot method. The amount of Ro 64-0802 effluxed to the buffer at time t [X_{buffer} (t), nanomoles per milligram of protein] can be described by the following equation:

$$dX_{buffer}(t)/dt = CL_{efflux} \times C_{cell}(t)$$

where CL_{efflux} (microliters per minute per milligram of protein) represents the efflux clearance of Ro 64-0802 from the cells, and C_{cell} (t) (micromolar concentration) is the cellular concentration of Ro 64-0802. Cellular volume was assumed to be 4 μl/mg protein. The integration of this equation from time 0 to time t yields the following equation:

$$X_{buffer}(t) = CL_{efflux} \times AUC_{cell}(0-t)$$

where AUC_{cell} (0–t) (micromolar concentration × min) represents the area under the cellular concentration-time curve for Ro 64-0802 from time 0 to time t. Because the amount of Ro 64-0802 in buffer [A_{buffer} (t), nanomoles per milligram of protein] is given by the sum of X_{buffer} (t) and the amount of Ro 64-0802 existing in the buffer at time 0 (X_0), A_{buffer} (t) is described by the following equation:

$$A_{buffer}(t) = CL_{efflux} \times AUC_{cell}(0-t) + X_0$$

Thus, the CL_{efflux} value can be obtained by fitting A_{buffer} (t) versus AUC_{cell} (0–t) using a least-squares regression program (MULTI) (Yamaoka et al., 1981).

Efflux of Ro 64-0802 from the Cerebral Cortex of Wild-Type, *Oat3*$^{-/-}$, and *Mrp4*$^{-/-}$ Mice after Microinjection. The efflux of the test compounds from the brain after their microinjection into the cerebral cortex was investigated using the brain efflux index method, as described previously (Kakee et al., 1996). Ro 64-0802 (1 mM) in 0.5 μl of ECF buffer (122 mM NaCl, 25 mM $NaHCO_3$, 10 mM *d*-glucose, 3 mM KCl, 1.4 mM $CaCl_2$, 1.2 mM $MgSO_4$, 0.4 mM K_2HPO_4, and 10 mM HEPES, pH 7.4) was injected into the cerebral cortex (4.5 mm lateral to the bregma and 2.5 mm in depth). After the intracerebral microinjection, the mice were decapitated, and the amount of Ro 64-0802 that remained in the ipsilateral cerebrum was determined with LC-MS analysis.

Brain/Plasma Concentration Ratio of Ro 64-0802 after Subcutaneous Infusion of Oseltamivir or Ro 64-0802 in Wild-Type, *Oat3*$^{-/-}$, and *Mrp4*$^{-/-}$ Mice. Male C57BL/6J, *Mrp4*$^{-/-}$, and *Oat3*$^{-/-}$ mice (10–18 weeks old), weighing approximately 25 to 30 g, were used for these experiments. An osmotic pump (8 μl/h; Alzet, Cupertino, CA) was implanted under the skin in the backs of the mice under pentobarbital anesthesia (30 mg/kg). The mice received a continuous subcutaneous infusion of oseltamivir or Ro 64-0802 at doses of 400 or 80 nmol/h/mouse, respectively. Blood samples were collected from the postcaval vein at 24 h after treatment under pentobarbital anesthesia, and the brain was excised immediately. Plasma was obtained by centrifugation of the blood samples (10,000g). The esterase inhibitor, dichlorvos (200 μg/ml), was used to prevent ex vivo hydrolysis of the oseltamivir to Ro 64-0802 in the blood and plasma (Wiltshire et al., 2000; Lindegardh et al., 2006). The plasma and brain concentrations of Ro 64-0802 were determined with LC-MS analysis.

Quantification of Ro 64-0802 in Plasma and Brain Specimens. The brain was homogenized with a 4-fold volume of phosphate-buffered saline to obtain a 20% brain homogenate. Plasma specimens (10 μl) were mixed with 40 μl of ethanol, and the brain homogenates (100 μl) were mixed with 400 μl of ethanol. All of these mixed solutions were centrifuged at 15,000g for 10 min. The supernatants of the plasma specimens were mixed with an equal volume of water and subjected to LC-MS analysis. The supernatants of the brain specimens (350 μl) were evaporated, and the pellets were reconstituted with 50 μl of 20% ethanol. The reconstituted specimens were centrifuged at 15,000g for 10 min, and an aliquot of the supernatant was subjected to LC-MS analysis.

An LCMS2010EV equipped with a Prominence LC system (Shimadzu, Kyoto, Japan) was used for the analysis. Samples were separated on a CAPCELL PAK C18 MGII column (3 μm, 2 mm × 50 mm; Shiseido, Tokyo, Japan) in binary gradient mode at a flow rate of 1 ml/min. Formic acid (0.05%) and acetonitrile were used for the mobile phase. The acetonitrile concentration was initially 10% and then increased linearly to 40% over 2 min. Finally, the column was reequilibrated at an acetonitrile concentration of 10% for 3 min. The total run time was 5 min. Ro 64-0802 was eluted at 2.5 min. In the mass analysis, Ro 64-0802 was detected at a mass-to-charge ratio of 285.15 under positive electron spray ionization conditions. The interface voltage was −3.5 kV, and the nebulizer gas (N_2) flow was 1.5 l/min. The heat block and curved desolvation line temperatures were 200 and 150°C, respectively.

Statistical Analysis. Data are presented as means ± S.E. of three to six animals, unless otherwise specified. Student's two-tailed unpaired t test and one-way ANOVA followed by Tukey's multiple comparison test were used to identify significant differences between groups when appropriate. Statistical significance was set at $P < 0.05$.

Results

Uptake of Ro 64-0802 into Human OAT3-Expressing HEK293 Cells. To show that Ro 64-0802 is an OAT3 substrate, an in vitro transport experiment was performed. The intracellular accumulation of Ro 64-0802 was significantly greater in HEK293 cells expressing human OAT3 than in mock-transfected cells (1.2 ± 0.2 and 15.1 ± 0.2 μl/10 min/mg protein for vector-transfected and OAT3-expressing HEK293 cells, respectively).

Construction of Human MRP4/CES1A1-Expressing MDCKII Cells. A clone of the MDCKII cells exogenously expressing CES1A1 was selected by measuring the hydrolytic activity against *p*-nitrophenyl acetate (data not shown). The subsequent study was performed using this clone as the host. After infection with the recombinant adenovirus, the protein expression of MRP4 in the MRP4/CES1A1-expressing MDCKII cells was confirmed by Western blot analysis (Fig. 1A). An anti-MRP4 monoclonal antibody recognized a 175-kDa protein, which is larger than the molecular mass for MRP4 (149 kDa) predicted from the sequence in the Swiss-Prot database. Deglycosylation of the cell lysates with *N*-glycosidase F resulted in a reduction in the molecular mass, suggesting that the molecular mass of MRP4 in the MRP4/CES1A1-expressing MDCKII cells was increased by glycosylation (Fig. 1B).

Efflux of Ro 64-0802 Formed Intracellularly from Oseltamivir in Human GFP/CES1A1 and MRP4/CES1A1-Expressing MDCKII Cells. An efflux transport experiment was conducted using MRP4/CES1A1- and GFP/CES1A1-MDCKII cells. When MRP4/CES1A1- and GFP/CES1A1-MDCKII cells were incubated with oseltamivir, Ro 64-0802 was detected in both the buffer and the cells in a time-dependent manner (Fig. 1, C and D). The concentration of Ro 64-0802 in the buffer was higher for the MRP4/CES1A1-MDCKII cells than for the GFP/CES1A1-MDCKII cells, and cellular Ro 64-0802 was lower in the MRP4/CES1-MDCKII cells (Fig. 1, C and D). Indomethacin, an inhibitor of MRP4 (Reid et al., 2003; Nozaki et al., 2007), reversed the effects of exogenous MRP4 expression. Integration plots of the efflux transport of Ro 64-0802 are shown in Fig. 2A. The efflux clearance of Ro 64-0802 from MRP4/CES1A1-MDCKII cells was 3.1-fold greater than that from GFP/CES1A1-MDCKII cells and was significantly inhibited by indomethacin (Fig. 2B).

Efflux of Ro 64-0802 from the Cerebral Cortex of Wild-Type and *Oat3*$^{-/-}$ Mice after Microinjection. Real-time PCR was performed to check the adaptive regulation of efflux transporters at the BBB of *Oat3*$^{-/-}$ mice. There were no significant differences in the mRNA expression of Mdr1a, Bcrp, Mrp4, organic anion transporter peptide 1a4 (Oatp1a4), or Oatp1c1 in the cerebral cortex, quantified by real-time PCR, between wild-type and *Oat3*$^{-/-}$ mice (data not shown).

To examine the involvement of Oat3 in the efflux transport of Ro 64-0802 across the BBB, Ro 64-0802 was directly injected into the mouse cerebral cortex, and the amount of Ro 64-0802 remaining in the brain was determined at 60 and 120 min after injection. The amount of Ro 64-0802 remaining in the brain was compared between wild-type and *Oat3*$^{-/-}$ mice (Fig. 3). As shown in Fig. 3, *Oat3*$^{-/-}$

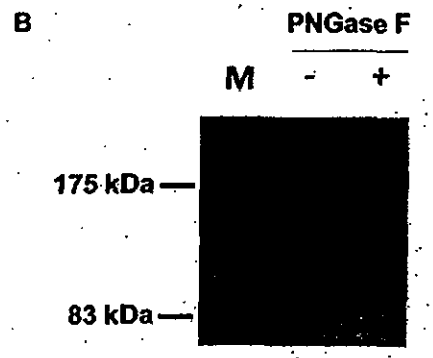

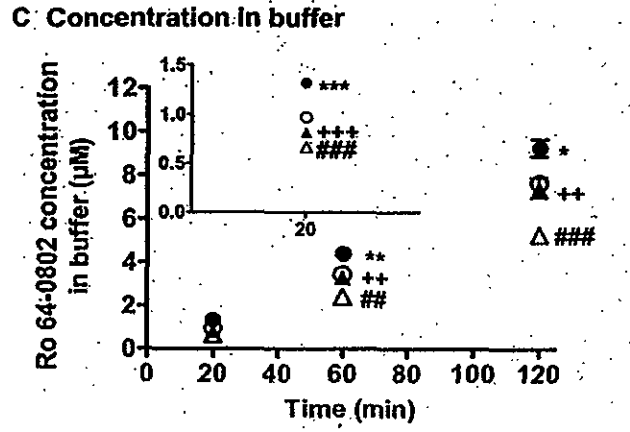

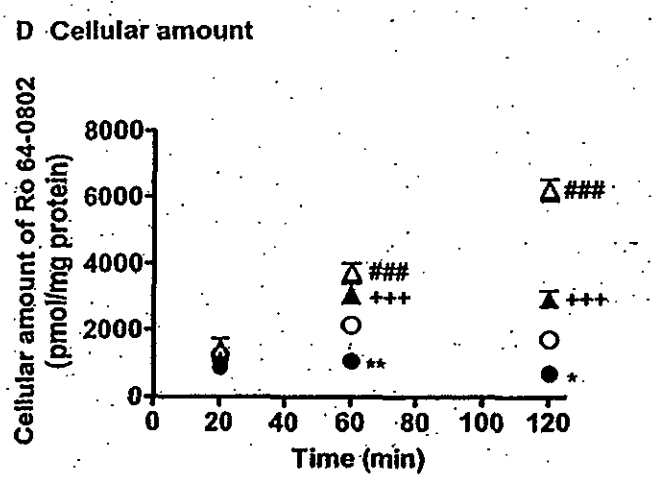

FIG. 1. Efflux of intracellularly formed Ro 64-0802 from mock-transfected and MRP4-expressing MDCKII cells. A and B, Western blotting. A, cell lysates were prepared from mock-transfected (GFP/CES1A1-MDCKII) and MRP4-expressing MDCKII cells (MRP4/CES1A1-MDCKII) and subjected to SDS-polyacrylamide gel electrophoresis (7.5%). B, *N*-linked carbohydrate groups were cleaved from the MRP4 protein in the cell lysates using *N*-glycosidase F (PNGase F). MRP4 was detected by the monoclonal anti-MRP4 M4I-10 antibody. C and D, efflux transport study: MRP4/CES1A1-MDCKII (●, ▲) and GFP/CES1A1-MDCKII cells (○, △) were incubated with 10 μM oseltamivir in the presence (▲, △) or absence (●, ○) of indomethacin (50 μM) at 37°C. Each point represents the mean ± S.E. ($n = 6$). Statistical significance was calculated by one-way ANOVA followed by Tukey's multiple comparison test. *, $P < 0.05$; **, $P < 0.01$; ***, $P < 0.001$; significantly different between MRP4/CES1A1-MDCKII and GFP/CES1A1-MDCKII cells. ##, $P < 0.01$; ###, $P < 0.001$; significantly different in GFP/CES1A1-MDCKII cells with and without indomethacin. ++, $P < 0.01$; +++, $P < 0.001$; significantly different in MRP4/CES1A1-MDCKII cells with and without indomethacin.

mice exhibited delayed elimination of Ro 64-0802 from the brain compared with that in wild-type mice.

Efflux of Ro 64-0802 from the Cerebral Cortex of Wild-Type and *Mrp4*$^{-/-}$ Mice after Microinjection. Real-time PCR was used to check the adaptive regulation of efflux transporters at the BBB of *Mrp4*$^{-/-}$ mice. No significant differences were observed in the mRNA expression levels of Mdr1a, Bcrp, Oat3, Oatp1a4, or Oatp1c1 in the cerebral cortex, quantified by real-time PCR, between wild-type and *Mrp4*$^{-/-}$ mice (data not shown).

To examine the involvement of Mrp4 in the efflux transport of Ro 64-0802 across the BBB, Ro 64-0802 was directly injected into the mouse cerebral cortex, and the amount of Ro 64-0802 remaining in the brain was determined at 60 and 120 min after injection. The amount of Ro 64-0802 remaining in the brain was compared between wild-type and *Mrp4*$^{-/-}$ mice (Fig. 4). As shown in Fig. 4, *Mrp4*$^{-/-}$ mice exhibited delayed elimination of Ro 64-0802 from the brain compared with that in wild-type mice.

Brain/Plasma Concentration Ratio of Ro 64-0802 after Subcutaneous Infusion of Oseltamivir or Ro 64-0802 in Wild-Type, *Oat3*$^{-/-}$, and *Mrp4*$^{-/-}$ Mice. To clarify the importance of the Oat3- and Mrp4-mediated efflux of Ro 64-0802 at the BBB, Ro 64-0802 was given to mice by subcutaneous infusion for 24 h, and the $K_{p,brain}$ of Ro 64-0802 was determined. The concentrations of Ro 64-0802 in

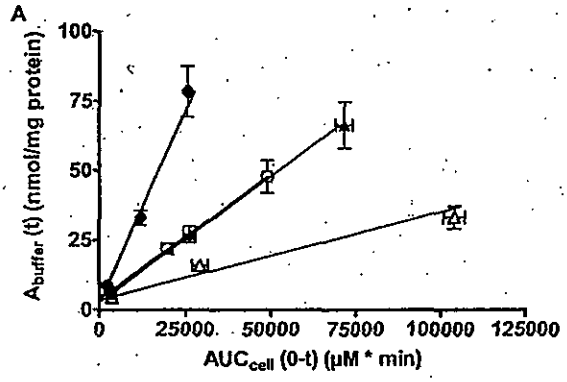

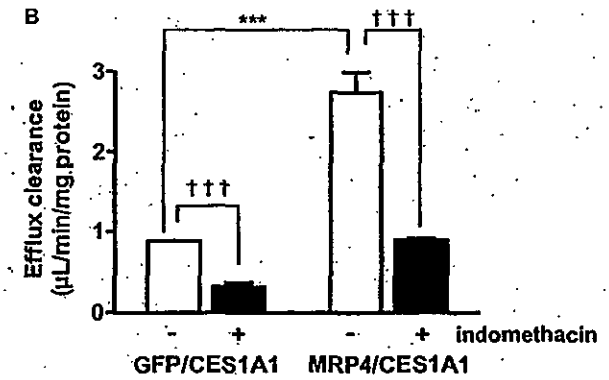

FIG. 2. Integration plots of the efflux transport of Ro 64-0802 from MRP4/CES1A1-MDCKII and GFP/CES1A1-MDCKII cells. A, integration plot: the amount of Ro 64-0802 in buffer [A_{buffer} (t)] was plotted against AUC_{cell} (0–t) in MRP4/CES1A1-MDCKII (●, ▲) and GFP/CES1A1-MDCKII cells (○, △) in the presence (▲, △) or absence (●, ○) of indomethacin (50 μM). The data used for the calculation are cited in Fig. 1, C and D. The slope of the plot represents the efflux clearance. Each point represents a mean ± S.E. ($n = 6$). B, efflux clearance of Ro 64-0802: The efflux clearance of Ro 64-0802 was calculated from the slope of the integration plot (A). Statistical significance was calculated by one-way ANOVA followed by Tukey's multiple comparison test. ***, $P < 0.001$; significantly different between MRP4/CES1A1-MDCKII and GFP/CES1A1-MDCKII cells. †††, $P < 0.001$; significantly different efflux clearance in the presence and absence of indomethacin. Data represent means ± computer-calculated S.D. (microliters per minute per milligram of protein).

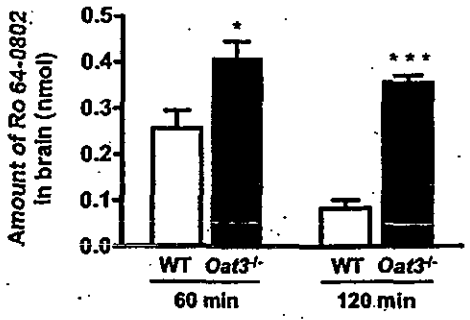

FIG. 3. Comparison of the amounts of Ro 64-0802 in the ipsilateral cerebrum after intracerebral microinjection of Ro 64-0802 in wild-type (WT) and *Oat3*$^{-/-}$ mice. *Ro 64-0802 (1 mM) in 0.5 μl of ECF buffer was injected into the Par2 region (4.5* mm lateral to the bregma and 2.5 mm in depth). The amount of Ro 64-0802 in the ipsilateral cerebrum was determined at 60 and 120 min after treatment. □, data for wild-type mice; ■, data for *Oat3*$^{-/-}$ mice. Each bar represents the mean ± S.E. *(n = 3–4). Statistically significant differences between wild-type and Oat3*$^{-/-}$ mice: *, $P < 0.05$; ***, $P < 0.001$.

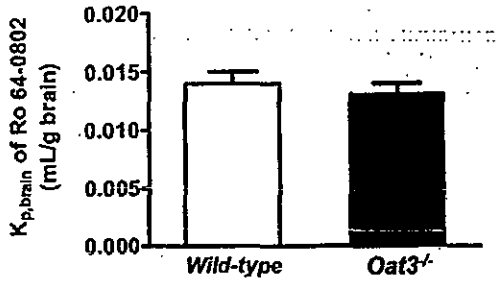

FIG. 5. Comparison of the brain/plasma concentration ratio ($K_{p,brain}$) of Ro 64-0802 after subcutaneous infusion of Ro 64-0802 in wild-type and *Oat3*$^{-/-}$ mice. Mice received a continuous subcutaneous infusion of Ro 64-0802 at a dose of 80 nmol/h/mouse for 24 h, with an osmotic pump. The plasma and brain concentrations of Ro 64-0802 were determined at 24 h after treatment. □, data for wild-type mice; ■, data for *Oat3*$^{-/-}$ mice. Each bar represents the mean ± S.E. (n = 3–4).

the plasma were 4.5 ± 0.6 and 4.5 ± 1.3 μM in wild-type and *Oat3*$^{-/-}$ mice, respectively. The $K_{p,brain}$ of Ro 64-0802 in *Oat3*$^{-/-}$ mice was not significantly different from that in wild-type mice and remained close to the capillary volume in the brain (Fig. 5). After subcutaneous infusions of oseltamivir in wild-type or *Mrp4*$^{-/-}$ mice, the plasma concentrations of Ro 64-0802 were 6.9 ± 2.3 and 12 ± 5 μM, respectively. The $K_{p,brain}$ of Ro 64-0802 was 3.8-fold higher in *Mrp4*$^{-/-}$ mice than that in wild-type mice (Fig. 6). Even after subcutaneous infusions of Ro 64-0802, the $K_{p,brain}$ of Ro 64-0802 was 6.4-fold greater in *Mrp4*$^{-/-}$ mice than that in wild-type mice (Fig. 6). The plasma concentrations of Ro 64-0802 were 5.7 ± 0.8 and 3.8 ± 1.7 μM in wild-type and *Mrp4*$^{-/-}$ mice treated with Ro 64-0802, respectively.

Discussion

Abnormal behavior is a suspected adverse effect of oseltamivir on the central nervous system. To understand the pharmacological action of oseltamivir in the brain, its uptake and efflux transport across the BBB were investigated as factors that determine its exposure to the central nervous system. In this study, we focused on Oat3 and Mrp4 as transporters of Ro 64-0802, a pharmacologically active form of oseltamivir, across the BBB.

First, we examined the involvement of Oat3 in the elimination of Ro 64-0802 from the cerebral cortex after microinjection because an in vitro transport study using OAT3-expressing HEK cells identified Ro 64-0802 as a substrate of OAT3. The elimination of Ro 64-0802 from the brain after its microinjection into the cerebral cortex was markedly delayed in *Oat3*$^{-/-}$ mice compared with wild-type mice (Fig. 3). This suggests that Oat3 plays a significant role in the efflux of Ro 64-0802 from the brain by facilitating its uptake from the brain interstitial space to endothelial cells. For the directional efflux of Ro 64-0802 from the brain to the blood across the BBB, a transporter(s) is also required to facilitate its luminal efflux, considering the hydrophilic nature of Ro 64-0802. In a previous study, we demonstrated that the brain concentrations of Ro 64-0802 in *Mdr1a/1b*$^{-/-}$ and *Abcg2*$^{-/-}$ mice are similar to that in wild-type mice (Ose et al., 2008), excluding the possibility that P-gp and Bcrp are involved in the luminal efflux of Ro 64-0802. Therefore, we focused on Mrp4, another ATP-binding cassette transporter at the BBB, as a candidate transporter because it has been reported to mediate the active efflux of topotecan and adefovir across the BBB (Leggas et al., 2004; Belinsky et al., 2007). To show that Ro 64-0802 is a substrate of MRP4, we constructed double transfectant cells expressing both CES1A1, an enzyme producing Ro 64-0802 from oseltamivir, and MRP4 (MRP4/CES1A1-MDCKII). The double transfectant exhibited enhanced efflux of Ro 64-0802 (which was inhibited by an MPR4 inhibitor, indomethacin) compared with GFP/CES1A1-MDCKII (Fig. 2B). It should be noted that the host cells also exhibited indomethacin-sensitive efflux of Ro 64-0802. This is presumably attributable to endogenous canine MRP4 because its mRNA expression was detected by reverse transcription-PCR in MDCKII cells (data not shown). The involvement of Mrp4 in the efflux of Ro 64-0802 across the BBB was

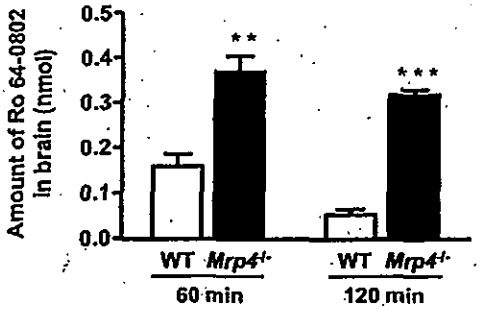

FIG. 4. Comparison of the amounts of Ro 64-0802 in the ipsilateral cerebrum after intracerebral microinjection of Ro 64-0802 in wild-type (WT) and *Mrp4*$^{-/-}$ mice. *Ro 64-0802 (1 mM) in 0.5 μl of ECF buffer was injected into the Par2 region (4.5* mm lateral to the bregma and 2.5 mm in depth). The amount of Ro 64-0802 in the ipsilateral cerebrum was determined at 60 and 120 min after treatment. □, data for wild-type mice; ■, data for *Mrp4*$^{-/-}$ mice. Each bar represents the mean ± S.E. *(n = 3–4). Statistically significant differences between wild-type and Mrp4*$^{-/-}$ mice: **, $P < 0.01$; ***, $P < 0.001$.

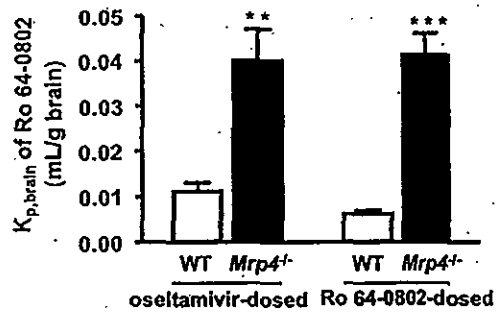

FIG. 6. Comparison of the brain/plasma concentration ratio ($K_{p,brain}$) of Ro 64-0802 after subcutaneous infusion of either oseltamivir or Ro 64-0802 in wild-type (WT) and *Mrp4*$^{-/-}$ mice. Mice received a continuous subcutaneous infusion of either *oseltamivir or Ro 64-0802 at a dose of 400 or 80 nmol/h/mouse, respectively, for* 24 h with an osmotic pump. The plasma and brain concentrations of Ro 64-0802 were determined at 24 h after treatment. □, data for wild-type mice; ■, data for *Mrp4*$^{-/-}$ mice. Each bar represents the mean ± S.E. (n = 4–6). Statistically *significant differences between wild-type and Mrp4*$^{-/-}$ mice: **, $P < 0.01$; ***, $P < 0.001$.

then examined using *Mrp4*$^{-/-}$ mice by microinjection into the cerebral cortex. *Mrp4*$^{-/-}$ mice exhibited delayed elimination of Ro 64-0802 from the cerebral cortex after its microinjection compared with that in wild-type mice (Fig. 4). Therefore, Mrp4 plays an important role in the luminal efflux of Ro 64-0802 after its cellular uptake by Oat3 from the brain side.

To show the importance of the active efflux of Ro 64-0802 at the BBB mediated by Oat3 and Mrp4, the $K_{p,\,brain}$ of Ro 64-0802 was determined in *Oat3*$^{-/-}$ or *Mrp4*$^{-/-}$ mice given Ro 64-0802 by subcutaneous infusion for 24 h. Our approach was based on the pharmacokinetic concept that reduced efflux across the BBB may lead to an increase in the $K_{p,\,brain}$. Consistent with a previous report (Ose et al., 2008), the $K_{p,\,brain}$ of Ro 64-0802 was close to the capillary volume in wild-type mice. The $K_{p,\,brain}$ of Ro 64-0802 observed in *Oat3*$^{-/-}$ mice was also close to the capillary volume (Fig. 5). In contrast, the $K_{p,\,brain}$ of Ro 64-0802 was 4- to 6-fold greater in *Mrp4*$^{-/-}$ mice than that in wild-type mice receiving either oseltamivir or Ro 64-0802 (Fig. 6). These in vivo results using *Mrp4*$^{-/-}$ mice thus indicate that Ro 64-0802 crosses the BBB from the blood side to the brain, but Mrp4 limits its penetration into the brain by extruding it into the blood. The latter finding is consistent with the results of our microinjection experiment. However, the lack of effect of knockout of *Oat3* on the $K_{p,\,brain}$ of Ro 64-0802 seems to contradict the results of the microinjection experiment. There are three explanations for this discrepancy. The first explanation is that luminal Mrp4 is more important in preventing brain penetration than abluminal Oat3. The second explanation is that, considering the mediation of bidirectional transport by Oat3 (Bakhiya et al., 2003), it is possible that Oat3 on the abluminal membrane of brain endothelial cells may act in the efflux of Ro 64-0802 from inside the endothelial cells into the brain, as well as in its uptake from the brain to the endothelial cells (Fig. 7). The third explanation is that, considering the hydrophilic character of Ro 64-0802, with an anionic charge, its luminal uptake probably involves transporters. Kikuchi et al. (2003) suggested that Oat3 is expressed on both the luminal and abluminal membranes of rat brain capillaries; however, this localization is controversial (Mori et al., 2003; Roberts et al., 2008). Oat3 may serve as an uptake system for Ro 64-0802 on the luminal membrane from the circulating blood into the brain (Fig. 7). Further studies using *Mrp4* and *Oat3* double knockout mice can answer these questions and perhaps confirm these speculations.

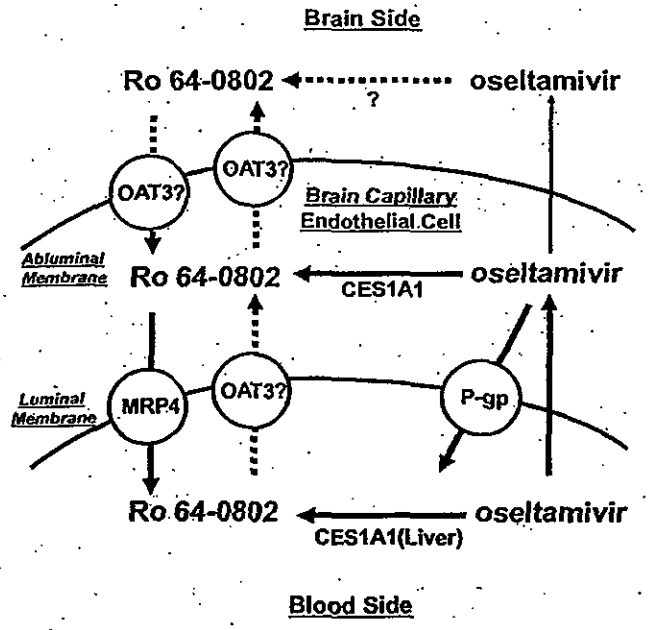

FIG. 7. Schematic representation of the proposed mechanism underlying the brain distribution of oseltamivir and Ro 64-0802 in humans. Oseltamivir crosses the BBB, and Ro 64-0802 is produced by CES1A1 during the penetration of oseltamivir across the BBB. Both oseltamivir and Ro 64-0802 are subjected to active efflux by P-gp and MRP4, respectively. The functional importance of OAT3 at the human BBB has not yet been established, so the hypothetical pathway is shown with a broken line.

Figure 7 summarizes the proposed mechanisms determining the brain distribution of oseltamivir and Ro 64-0802 in humans. P-gp, MRP4, and CES1A1 are factors that determine the brain distribution of oseltamivir and Ro 64-0802 in humans. CES1A1 is predominantly expressed in the brain capillaries in human brain (Yamada et al., 1994), although whether CES1A1 is the only enzyme responsible for the conversion of oseltamivir remains to be examined. MRP4 is also expressed on the luminal membranes of human brain capillaries (Nies et al., 2004; Bronger et al., 2005). Because oseltamivir crosses the BBB, Ro 64-0802 can be produced during the penetration of oseltamivir across the BBB and then be subjected to active efflux by MRP4. Although Northern blotting did detect OAT3 mRNA expression in the human brain (Cha et al., 2001), its distribution and membrane localization remain to be determined. Therefore, whether Ro 64-0802 can penetrate into the brain and is eliminated from the brain by OAT3 in humans, as well as in mice, also remains in question. Fluctuations in their activities will cause interindividual variations in their exposure to the central nervous system. For instance, genetic variations have been reported for P-gp and MRP4, which may alter their transport activities and expression. The silent mutation 3435C>T is associated with reduced P-gp expression (Hoffmeyer et al., 2000) and affects protein folding, resulting in a substrate-dependent functional change (Kimchi-Sarfaty et al., 2007). In MRP4, the nonsynonymous mutations 559G>T, 1460G>A, and 2269G>A are associated with altered transport activity and expression (Abla et al., 2008; Krishnamurthy et al., 2008). It is possible that these polymorphisms are associated with the adverse effects of Ro 64-0802 on the central nervous system.

In conclusion, Mrp4 and Oat3 are responsible for the elimination of Ro 64-0802 from the brain across the BBB although, at steady-state, Oat3 may not affect its brain distribution, probably because of its possible contribution also to the brain uptake of Ro 64-0802. This is the first demonstration of the cooperation of uptake and efflux transporters in the directional (brain-to-blood) transport of anionic drugs across the BBB.

Acknowledgments. We thank Dr. Junko Iida and Futoshi Kurotobi (Shimadzu) for technical support with the LC-MS system.

References

Abla N, Chinn LW, Nakamura T, Liu L, Huang CC, Johns SJ, Kawamoto M, Stryke D, Taylor TR, Ferrin TE, Giacomini KM, and Kroetz DL (2008) The human multidrug resistance protein 4 (MRP4, *ABCC4*): functional analysis of a highly polymorphic gene. *J Pharmacol Exp Ther* 325:859–868.

Bakhiya A, Bahn A, Burckhardt G, and Wolff N (2003) Human organic anion transporter 3 (hOAT3) can operate as an exchanger and mediate secretory urate flux. *Cell Physiol Biochem* 13:249–256.

Bardsley-Elliot A and Noble S (1999) Oseltamivir. *Drugs* 58:851–860; discussion 861–862.

Belinsky MG, Guo P, Lee K, Zhou F, Kotova E, Grinberg A, Westphal H, Shchaveleva I, Klein-Szanto A, Gallo JM, et al. (2007) Multidrug resistance protein 4 protects bone marrow, thymus, spleen, and intestine from nucleotide analogue-induced damage. *Cancer Res* 67:262–268.

Bronger H, König J, Kopplow K, Steiner HH, Ahmadi R, Herold-Mende C, Keppler D, and Nies AT (2005) ABCC drug efflux pumps and organic anion uptake transporters in human gliomas and the blood-tumor barrier. *Cancer Res* 65:11419–11428.

Cha SH, Sekine T, Fukushima JI, Kanai Y, Kobayashi Y, Goya T, and Endou H (2001) Identification and characterization of human organic anion transporter 3 expressing predominantly in the kidney. *Mol Pharmacol* 59:1277–1286.

Ci L, Kusuhara H, Adachi M, Schuetz JD, Takeuchi K, and Sugiyama Y (2007) Involvement of MRP4 (ABCC4) in the luminal efflux of ceftizoxime and cefazolin in the kidney. *Mol Pharmacol* 71:1591–1597.

Deguchi T, Kusuhara H, Takadate A, Endou H, Otagiri M, and Sugiyama Y (2004) Characterization of uremic toxin transport by organic anion transporters in the kidney. *Kidney Int* 65:162–174.

Fuyuno I (2007) Tamiflu side effects come under scrutiny. *Nature* 446:358–359.

Hasegawa M, Kusuhara H, Adachi M, Schuetz JD, Takeuchi K, and Sugiyama Y (2007) Multidrug resistance-associated protein 4 is involved in the urinary excretion of hydrochlorothiazide and furosemide. *J Am Soc Nephrol* 18:37–45.

He G, Massarella J, and Ward P (1999) Clinical pharmacokinetics of the prodrug oseltamivir and its active metabolite Ro 64-0802. *Clin Pharmacokinet* 37:471–484.

Hill G, Cihlar T, Oo C, Ho ES, Prior K, Wiltshire H, Barrett J, Liu B, and Ward P (2002) The anti-influenza drug oseltamivir exhibits low potential to induce pharmacokinetic drug interactions via renal secretion-correlation of in vivo and in vitro studies. *Drug Metab Dispos* 30:13–19.

Hoffmeyer S, Burk O, von Richter O, Arnold HP, Brockmöller J, Johne A, Cascorbi I, Gerloff T, Roots I, Eichelbaum M, et al. (2000) Functional polymorphisms of the human multidrug-resistance gene: multiple sequence variations and correlation of one allele with P-glycoprotein expression and activity in vivo. *Proc Natl Acad Sci U S A* 97:3473–3478.

Imaoka T, Kusuhara H, Adachi M, Schuetz JD, Takeuchi K, and Sugiyama Y (2007) Functional involvement of multidrug resistance-associated protein 4 (MRP4/ABCC4) in the renal elimination of the antiviral drugs adefovir and tenofovir. *Mol Pharmacol* 71:619–627.

Izumi Y, Tokuda K, O'dell KA, Zorumski CF, and Narahashi T (2007) Neuroexcitatory actions of Tamiflu and its carboxylate metabolite. *Neurosci Lett* 426:54–58.

Kakee A, Terasaki T, and Sugiyama Y (1996) Brain efflux index as a novel method of analyzing efflux transport at the blood-brain barrier. *J Pharmacol Exp Ther* 277:1550–1559.

Kikuchi R, Kusuhara H, Abe T, Endou H, and Sugiyama Y (2004) Involvement of multiple transporters in the efflux of 3-hydroxy-3-methylglutaryl-CoA reductase inhibitors across the blood-brain barrier. *J Pharmacol Exp Ther* 311:1147–1153.

Kikuchi R, Kusuhara H, Sugiyama D, and Sugiyama Y (2003) Contribution of organic anion transporter 3 (Slc22a8) to the elimination of p-aminohippuric acid and benzylpenicillin across the blood-brain barrier. *J Pharmacol Exp Ther* 306:51–58.

Kimchi-Sarfaty C, Oh JM, Kim IW, Sauna ZE, Calcagno AM, Ambudkar SV, and Gottesman MM (2007) A "silent" polymorphism in the MDR1 gene changes substrate specificity. *Science* 315:525–528.

Krishnamurthy P, Schwab M, Takenaka K, Nachagari D, Morgan J, Leslie M, Du W, Boyd K, Cheok M, Nakauchi H, et al. (2008) Transporter-mediated protection against thiopurine-induced hematopoietic toxicity. *Cancer Res* 68:4983–4989.

Leggas M, Adachi M, Scheffer GL, Sun D, Wielinga P, Du G, Mercer KE, Zhuang Y, Panetta JC, Johnston B, et al. (2004) Mrp4 confers resistance to topotecan and protects the brain from chemotherapy. *Mol Cell Biol* 24:7612–7621.

Lindegardh N, Davies GR, Tran TH, Farrar J, Singhasivanon P, Day NP, and White NJ (2006) Rapid degradation of oseltamivir phosphate in clinical samples by plasma esterases. *Antimicrob Agents Chemother* 50:3197–3199.

Lowry OH, Rosebrough NJ, Farr AL, and Randall RJ (1951) Protein measurement with Folin phenol reagent. *J Biol Chem* 193:265–267.

Mori M, Hosokawa M, Ogasawara Y, Tsukada E, and Chiba K (1999) cDNA cloning, characterization and stable expression of novel human brain carboxylesterase. *FEBS Lett* 458:17–22.

Mori S, Ohtsuki S, Takanaga H, Kikkawa T, Kang YS, and Terasaki T (2004) Organic anion transporter 3 is involved in the brain-to-blood efflux transport of thiopurine nucleobase analogs. *J Neurochem* 90:931–941.

Mori S, Takanaga H, Ohtsuki S, Deguchi T, Kang YS, Hosoya K, and Terasaki T (2003) Rat organic anion transporter 3 (rOAT3) is responsible for brain-to-blood efflux of homovanillic acid at the abluminal membrane of brain capillary endothelial cells. *J Cereb Blood Flow Metab* 23:432–440.

Morimoto K, Nakakariya M, Shirasaka Y, Kakinuma C, Fujita T, Tamai I, and Ogihara T (2008) Oseltamivir (Tamiflu) efflux transport at the blood-brain barrier via P-glycoprotein. *Drug Metab Dispos* 36:6–9.

Nies AT, Jedlitschky G, König J, Herold-Mende C, Steiner HH, Schmitt HP, and Keppler D (2004) Expression and immunolocalization of the multidrug resistance proteins, MRP1–MRP6 (ABCC1–ABCC6), in human brain. *Neuroscience* 129:349–360.

Nozaki Y, Kusuhara H, Kondo T, Iwaki M, Shiroyanagi Y, Nakayama H, Horita S, Nakazawa H, Okano T, and Sugiyama Y (2007) Species difference in the inhibitory effect of nonsteroidal anti-inflammatory drugs on the uptake of methotrexate by human kidney slices. *J Pharmacol Exp Ther* 322:1162–1170.

Ohtsuki S, Asaba H, Takanaga H, Deguchi T, Hosoya K, Otagiri M, and Terasaki T (2002) Role of blood-brain barrier organic anion transporter 3 (OAT3) in the efflux of indoxyl sulfate, a uremic toxin: its involvement in neurotransmitter metabolite clearance from the brain. *J Neurochem* 83:57–66.

Ose A, Kusuhara H, Yamatsugu K, Kanai M, Shibasaki M, Fujita T, Yamamoto A, and Sugiyama Y (2008) P-glycoprotein restricts the penetration of oseltamivir across the blood-brain barrier. *Drug Metab Dispos* 36:427–434.

Reid G, Wielinga P, Zelcer N, van der Heijden I, Kuil A, de Haas M, Wijnholds J, and Borst P (2003) The human multidrug resistance protein MRP4 functions as a prostaglandin efflux transporter and is inhibited by nonsteroidal antiinflammatory drugs. *Proc Natl Acad Sci U S A* 100:9244–9249.

Roberts LM, Black DS, Raman C, Woodford K, Zhou M, Haggerty JE, Yan AT, Cwirla SE, and Grindstaff KK (2008) Subcellular localization of transporters along the rat blood-brain barrier and blood-cerebral-spinal fluid barrier by in vivo biotinylation. *Neuroscience* 155:423–438.

Satoh K, Nonaka R, Ogata A, Nakae D, and Uehara S (2007) Effects of oseltamivir phosphate (Tamiflu) and its metabolite (GS4071) on monoamine neurotransmission in the rat brain. *Biol Pharm Bull* 30:1816–1818.

Shi D, Yang J, Yang D, LeCluyse EL, Black C, You L, Akhlaghi F, and Yan B (2006) Anti-influenza prodrug oseltamivir is activated by carboxylesterase human carboxylesterase 1, and the activation is inhibited by antiplatelet agent clopidogrel. *J Pharmacol Exp Ther* 319:1477–1484.

Usami A, Sasaki T, Satoh N, Akiba T, Yokoshima S, Fukuyama T, Yamatsugu K, Kanai M, Shibasaki M, Matsuki N, et al. (2008) Oseltamivir enhances hippocampal network synchronization. *J Pharmacol Sci* 106:659–662.

Wiltshire H, Wiltshire B, Citron A, Clarke T, Serpe C, Gray D, and Herron W (2000) Development of a high-performance liquid chromatographic-mass spectrometric assay for the specific and sensitive quantification of Ro 64-0802, an anti-influenza drug, and its pro-drug, oseltamivir, in human and animal plasma and urine. *J Chromatogr B Biomed Sci Appl* 745:373–388.

Yamada T, Hosokawa M, Satoh T, Moroo I, Takahashi M, Akatsu H, and Yamamoto T (1994) Immunohistochemistry with an antibody to human liver carboxylesterase in human brain tissues. *Brain Res* 658:163–167.

Yamaoka K, Tanigawara Y, Nakagawa T, and Uno T (1981) A pharmacokinetic analysis program (multi) for microcomputer. *J Pharmacobiodyn* 4:879–885.

Yamatsugu K, Kamijo S, Suto Y, Kanai M, and Shibasaki M (2007) A concise synthesis of Tamiflu: third generation route via the Diels-Alder reaction and the Curtius rearrangement. *Tetrahedron Lett* 48:1403–1406.

Yoshino T, Nisijima K, Shioda K, Yui K, and Kato S (2008) Oseltamivir (Tamiflu) increases dopamine levels in the rat medial prefrontal cortex. *Neurosci Lett* 438:67–69.

Address correspondence to: Dr. Yuichi Sugiyama, Department of Molecular Pharmacokinetics, Graduate School of Pharmaceutical Sciences, The University of Tokyo, 7-3-1 Hongo, Bunkyo-ku, Tokyo 113-0033, Japan. E-mail: sugiyama@mol.f.u-tokyo.ac.jp

BIOCHEMICAL PHARMACOLOGY 77 (2009) 238–247

available at www.sciencedirect.com

ScienceDirect

journal homepage: www.elsevier.com/locate/biochempharm

Human carboxylesterases HCE1 and HCE2: Ontogenic expression, inter-individual variability and differential hydrolysis of oseltamivir, aspirin, deltamethrin and permethrin☆

Dongfang Yang[a], *Robin E. Pearce*[b], *Xiliang Wang*[a], *Roger Gaedigk*[b], *Yu-Jui Yvonne Wan*[c], *Bingfang Yan*[a,*]

[a] *Department of Biomedical and Pharmaceutical Sciences, Center for Pharmacogenomics and Molecular Therapy, University of Rhode Island Kingston, Kingston, RI 02881, United States*

[b] *Section of Developmental Pharmacology and Experimental Therapeutics, Division of Pediatric Pharmacology and Medical Toxicology, Children's Mercy Hospital and Clinics, 2401 Gillham Road, Kansas City, MO 64108, United States*

[c] *Department of Pharmacology, Toxicology and Therapeutics, University of Kansas Medical Center, Kansas City, KS 66160, United States*

ARTICLE INFO

Article history:
Received 7 September 2008
Accepted 6 October 2008

ABSTRACT

Carboxylesterases hydrolyze chemicals containing such functional groups as a carboxylic acid ester, amide and thioester. The liver contains the highest carboxylesterase activity and expresses two major carboxylesterases: HCE1 and HCE2. In this study, we analyzed 104 individual liver samples for the expression patterns of both carboxylesterases. These samples were divided into three age groups: adults (≥ 18 years of age), children (0 days–10 years) and fetuses (82–224 gestation days). In general, the adult group expressed significantly higher HCE1 and HCE2 than the child group, which expressed significantly higher than the fetal group. The age-related expression was confirmed by RT-qPCR and Western immunoblotting. To determine whether the expression patterns reflected the hydrolytic activity, liver microsomes were pooled from each group and tested for the hydrolysis of drugs such as oseltamivir and insecticides such as deltamethrin. Consistent with the expression patterns, adult microsomes were ~4 times as active as child microsomes and 10 times as active as fetal microsomes in hydrolyzing these chemicals. Within the same age group, particularly in the fetal and child groups, a large inter-individual variability was detected in mRNA (430-fold), protein (100-fold) and hydrolytic activity (127-fold). Carboxylesterases are recognized to play critical roles in drug metabolism and insecticide detoxication. The findings on the large variability among different age groups or even within the same age group have important pharmacological and toxicological implications, particularly in relation to pharmacokinetic alterations of ester drugs in children and vulnerability of fetuses and children to pyrethroid insecticides.

☆ This work was supported by NIH grants R01ES07965 and R01GM61988 (BY) and R01CA053596 (YJW).

* *Corresponding author.* Tel.: +1 401 874 5032; fax: +1 401 874-5048.
E-mail address: byan@uri.edu (B. Yan).

Abbreviations: GAPDH, glyceradehyde-3-phosphate dehydrogenase; HCE, human carboxylesterase; HPLC, high-performance liquid chromatography; PBS, phosphate buffered saline; RT-qPCR, reverse transcription-quantitative polymerase chain reaction.

0006-2952/$ – see front matter © 2008 Elsevier Inc. All rights reserved.
doi:10.1016/j.bcp.2008.10.005

1. Introduction

Carboxylesterases constitute a class of enzymes that hydrolyze chemicals containing such functional groups as a carboxylic acid ester, amide and thioester [1]. These enzymes are known to play important roles in drug metabolism and insecticide detoxication. Two major human carboxylesterases (HCE1 and HCE2) are abundantly expressed in the liver, whereas HCE2 is predominately expressed in the gastrointestinal tract [1,2]. In addition to the difference in tissue distribution, these two enzymes differ markedly in the hydrolysis of certain drugs. For example, HCE1, but not HCE2, rapidly hydrolyzes the anti-influenza viral agent oseltamivir [3,4]. In contrast, HCE2, but not HCE1, rapidly hydrolyzes the anticancer agent irinotecan [5]. In addition to hydrolyzing numerous compounds, carboxylesterases catalyze transesterification. In the presence of ethyl alcohol, HCE1 effectively converts the anti-platelet agent clopidogrel (a methyl ester) into ethyl clopidogrel [4].

The expression of carboxylesterase is altered by xenobiotics and pathological conditions. In human primary hepatocytes, therapeutic agents such as dexamethasone and phenobarbital cause a slight or moderate induction of HCE1 and HCE2 [6]. Dexamethasone and phenobarbital also alter the expression of rat carboxylesterases [7]. However, the pattern of the alteration is different. Phenobarbital moderately induces rat carboxylesterases (hydrolase A and hydrolase B), whereas dexamethasone profoundly suppresses the expression of these enzymes [7]. Suppression also occurs in human primary hepatocytes treated with the pro-inflammatory cytokine interleukin-6 (IL-6), and the suppression is achieved by transcriptional repression [8]. More importantly, the IL-6 mediated suppression strongly alters cellular responsiveness to therapeutic agents such as clopidogrel, irinotecan, and oseltamivir [8]. Hydrolysis of clopidogrel represents inactivation. In contrast, hydrolysis of irinotecan and oseltamivir leads to the formation of therapeutically active metabolites thus represents activation [5,9].

The expression of carboxylesterases is regulated in a developmental manner, and it seems likely that these enzymes are developmentally regulated in humans as well. One to two week old rats express no hydrolase A or B based on immunoblotting analysis [7]. Consistent with the low level expression of carboxylesterases, the intrinsic clearance of the pyrethroid deltamethrin through hydrolysis in 10-day-old rats is only ~3% of adult rats [10]. Even in 4-week-old rats, the intrinsic clearance is less than half of that of adult rats [10]. In addition, young animals are generally much more sensitive to pesticides such as organophosphates and pyrethroids [11–13]. Carboxylesterases are known to protect against these chemicals by hydrolysis in the case of pyrethroids or scavenging mechanism in the case of organophoaphates. The developmental regulation of human carboxylesterases remains to be established. A previous report by Pope et. al. [14] observed that infants differ from adults in the expression and hydrolytic activity of carboxylesterases, but the difference was statistically insignificant [14]. The Pope's study, however, used a small number of samples and had only five samples for each group.

In the current study, we analyzed a total of 104 individual liver samples for the expression patterns of HCE1 and HCE2. These samples were grouped according to age: adults (>18 years old), children (0–10) and fetuses. Multiple experimental approaches were used including RT-qPCR, Western analysis and enzymatic assays. The fetuses expressed lower carboxylesterases than the children, and the children expressed lower carboxylesterases than the adults. Overall, the expression of both HCE1 and HCE2 showed a large inter-individual variability with the largest variability in the fetal group.

2. Materials and methods

2.1. Chemicals and supplies

Acetaminophen, aspirin, naproxen, and salicylic acid were purchased from Sigma (St. Louis, MO). Clopidogrel and clopidogrel carboxylate were from ChemPacific (Baltimore, MD). Oseltamivir and oseltamivir carboxylate were from Toronto Research Chemicals (Canada). Deltamethrin and permethrin were purchased from ChemService (West Chester, PA). Deltamethrin had a purity of 99%, and permethrin was from a batch that contained a mixture of cis- and trans-isomers at a ratio of 46% and 52%, respectively. TaqMan probes were from Applied Biosystems (Foster City, CA). The antibody against glyceradehyde-3-phosphate dehydrogenase (GAPDH) was from Abcam (Cambridge, MA). Unless otherwise specified, all other reagents were purchased from Fisher Scientific (Pittsburgh, PA).

2.2. Liver RNA and microsomal samples

A total of 104 RNA samples were used in this study and some of the RNA samples were matched with microsomes. Pure RNA samples were purchased from (ADMET Technologies (Durham, NC). Liver tissues were acquired from the National Disease Research Interchange (Philadelphia, PA), the Midwest Transplant Network (Westwood, KS), the University of Maryland Brain and Tissue Bank for Developmental Disorders (Baltimore, MD), and the University of Washington Central Laboratory for Human Embryology (Seattle, WA). Isolation of total RNA from the liver tissues was described previously [15,16], and the quality was determined on an Experion RNA StdSens micro fluidic chip (Bio-Rad, Hercules, CA) or by electrophoresis. Microsomes of child and fetal livers were prepared by differential centrifugation as described previously [17]. Adult liver microsomes (individual samples) were from CellzDirect (Pittsboro, NC) and described previously [4]. The demographics of the RNA samples in each group are summarized in Table 1. The use of the human samples was approved by the Institutional Review Board.

Table 1 – Demographic data for RNA samples.

Group	n	M/F	CA	AA	H	Others	Unk
Fetus	48	26/22	19	17	1	5	6
Child	34	15/19	21	8	3	2	
Adult	22	14/8	19	2			

Abbreviations: M/F: male/female; CA: Caucasian-American; AA: African American; H: Hispanic; Unk: unknown.

2.3. Reverse transcription-quantitative polymerase chain reaction (RT-qPCR)

Total RNA (0.1 μg) was subjected to the synthesis of the first strand cDNA in a total volume of 25 μl with random primers and M-MLV reverse transcriptase. The reactions were conducted at 25 °C for 10 min, 42 °C for 50 min and 70 °C for 10 min. The cDNAs were then diluted 6-fold and quantitative PCR was performed with TaqMan Gene Expression Assay (Applied Biosystems, Foster City, CA). The TaqMan assay identification numbers were: HCE1, Hs00275607_m1 (NM_001266); HCE2, Hs00187279_m1 (NM_198061); and polymerase (RNA) II, Hs01108291_m1 (NM_000937). It should be noted that the HCE1 probe could detect both HCE1A1 and HCE1A2 transcripts. The PCR amplification was conducted in a total volume of 20 μl containing universal PCR master mixture (10 μl), gene-specific TaqMan assay mixture (1 μl), and cDNA template (3 μl). The cycling profile was 50 °C for 2 min, 95 °C for 10 min, followed by 40 cycles of 15 s at 95 °C and 1 min at 60 °C, as recommended by the manufacturer. Amplification and quantification were done with the Applied Biosystems 7900HT Real-Time PCR System. All samples were analyzed in triplicate and the signals were normalized to polymerase (RNA) II [18] and then expressed as relative levels of mRNA among all samples.

2.4. Western analysis

Microsomal proteins (1.5 μg) were resolved by 7.5% SDS-PAGE in a mini-gel apparatus and transferred electrophoretically to nitrocellulose membranes. After non-specific binding sites were blocked with 5% non-fat milk, the blots were incubated with an antibody against HCE1, HCE2 and GAPDH, respectively. The preparation of the antibodies against HCE1 and HCE2 was described elsewhere [6]. The primary antibodies were subsequently localized with goat anti-rabbit IgG conjugated with horseradish peroxidase, and horseradish peroxidase activity was detected with a chemiluminescent kit (SuperSignal West Pico). The chemiluminescent signals were captured by a KODAK Image Station 2000 and the relative intensities were quantified by the KODAK 1D Image Analysis Software.

2.5. Enzymatic assays

All enzymatic assays were carried out at 37 °C in a total volume of 100 μl. Pilot studies were performed to determine conditions (e.g., protein concentrations) to maintain the metabolism in the linear range. Generally, microsomes (20–80 μg protein) were prepared in 50 μl incubation buffer (phosphate buffer, 100 mM, pH 7.4; or Tris–HCl, 50 mM, pH 7.4) and then mixed with an equal volume of substrate solution (the same buffer). Hydrolysis of aspirin was performed in phosphate buffer, whereas hydrolysis of oseltamivir, deltamethrin and permethrin was carried out in Tris–HCl buffer. Aspirin was assayed at 1 mM, oseltamivir at 200 μM, both deltamethrin and permethrin at 100 μM. The incubations lasted for 10–60 min depending on a substrate, and the reactions were terminated with 150 μl of acetonitrile containing an internal standard (IS): acetaminophen (750 ng/ml) for aspirin, clopidogrel carboxylate (50 ng/ml) for oseltamivir, napronex (4 μg/ml) for deltamethrin and clopidogrel (33 μg/ml) for permethrin. The reaction mixtures were subjected to centrifugation for 15 min at 4 °C (15,000 *g*). Hydrolysis of aspirin and oseltamivir was previously reported [3,4]. It should be noted that various controls were performed such as 0 min incubation and incubation without microsomes.

2.6. Monitoring of hydrolysis by HPLC or LC–MS/MS

The hydrolysis of aspirin or pyrethroids was separated by high-performance liquid chromatography (HPLC) (Hitachi LaChrom Elite-300) with a Chromolith SpeedROD column RP-18e (Merck, Germany). The supernatants (10–30 μl) of the reaction mixtures were injected and separated by an isocratic for aspirin or gradient mobile phase for deltamethrin and permethrin. The isocratic mobile phase consisted of 12% methanol and 0.25% acetate acid at pH 3.9 [4]. The gradient mobile phase consisted of acetonitrile and 0.01% formic acid. The gradient was run at 20–50% acetonitrile (v/v) for 6 min, 50–80% for 3 min followed by 80–20% for 6 min. Both mobile phases were run at a flow rate of 2 ml/min. For aspirin, the formation of hydrolytic metabolite was monitored, whereas for deltamethrin and permethrin the disappearance of parent compounds was monitored by a diode array detector at 230 nm. All quantifications were performed using peak area ratios and calibration curves generated from the internal control. The calibration curve ranged from 2 to 300 μg/mL with good linearity for salicylic acid, 0.8–160 μg/mL for deltamethrin, and 0.6–120 μg/mL for permethrin.

The hydrolysis of oseltamivir was monitored by LC–MS/MS system (API 3200) as described previously [3]. Briefly, the supernatants of the incubation mixtures were separated isocratically using a mobile phase composition of 70:30% (v/v) acetonitrile: 0.05% (v/v) formic acid in deionized water maintained at a flow rate of 0.25 ml/min with a total run time of 6.0 min. Detection of the analytes was performed in positive ion mode using the mass transitions of *m/z*: 313.3 → 166.1 for oseltamivir, *m/z*: 285.2 → 138.0 for oseltamivir carboxylate and *m/z*: 308.2 → 152.0 for IS. Flow injection analysis was performed at a flow rate of 20 μl/min to obtain optimum source parameters. The following compound parameters were used for oseltamivir, oseltamivir carboxylate and IS, respectively. Declustering potential: +5, +5 and +30 V, focusing potential: +360 V each, entrance potential: +8 V each, collision cell entrance potential: +20 V each, collision energy: +25, +25 and +30 V and collision cell exit potential: +7 V each. The optimum source parameters that gave the highest oseltamivir intensity were Curtain gas: 10 psi, collision gas: 4 psi, ion spray voltage: +5500 V, temperature: 450 °C, ion source gas1: 25 psi and ion source gas2: 85 psi. Integration of the peaks was performed by manual baseline adjustment using the ANALYST SP version 1.2 software (Applied Biosystems). All quantifications were performed using peak area ratios and calibration curves consisted of oseltamivir or oseltamivir carboxylate to clopidogrel carboxylic acid concentration ratios plotted against the oseltamivir or oseltamivir carboxylate to clopidogrel carboxylic acid peak area ratios. The calibration curve ranged from 1 to 250 ng/mL with good linearity for oseltamivir and 4 to 1000 ng/mL for oseltamivir carboxylate.

The calibration curves were constructed with $1/x^2$ weighting and the regression coefficients were greater than 0.99.

2.7. Other analyses

Protein concentrations were determined with BCA assay (Pierce) based on bovine serum albumin standard. Data are presented as mean ± S.D. All enzymatic assays were repeated three times with the same microsomal preparation. Statistical tests were performed to compare means (Student's t-test) or correlations (Spearman). In all cases, significant differences were assumed when p-values were less than 0.05.

3. Results

3.1. Ontogenic expression of human carboxylesterases HCE1 and HCE2 by RT-qPCR

In this study, we first evaluated the expression patterns of human carboxylesterases HCE1 and HCE2 in various age groups. A total of 104 RNA samples were analyzed including 48 samples from fetuses (82–224 gestation days), 34 from children (0 days–10 years of age) and 22 from adults (≥18). The levels of HCE1 and HCE2 mRNA were determined with RT-qPCR, and the results are summarized in Fig. 1 and Table 2. Overall, the adult group had the highest levels of HCE1 and HCE2 mRNA, and the fetal group had the lowest levels for both enzymes. Based on the values of the means, the adult group expressed HCE1 at levels 319-fold higher than the fetal group, and ~50% higher than the child group (Fig. 1 and Table 2). Likewise, the adult group expressed HCE2 at levels 55-fold higher than the fetal group and ~40% higher than the child group. In all cases, the differences among various age groups were statistically significant (Fig. 1). It should be noted that two different sets of Y axial values were used in Fig. 1 to accommodate the large difference in the mRNA levels between the fetal and the other two groups.

In addition to the large difference among various age groups (inter-group), a large inter-individual variability was detected within a group. The fetal group, for example, showed a 431-fold difference (ratio between the maximum and the minimum) in HCE1 mRNA with a coefficient of variation (CV) of as high as 172% (Table 2). The child and adult groups, on the other hand, varied less in HCE1 mRNA with a 218- and 12-fold difference, respectively (Table 2). Similarly, the levels of HCE2 mRNA varied in all age groups, however, the overall variability was much less than HCE1 mRNA. The variation in HCE2 mRNA

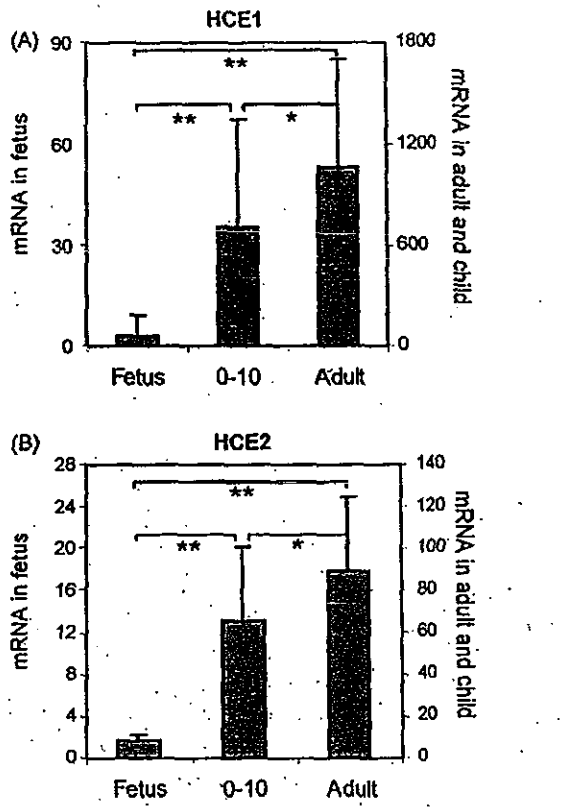

Fig. 1 – Levels of HCE1 and HCE 2 mRNA in the adult, child and fetal groups. Total RNAs were subjected to RT-qPCR analysis for the level of HCE1 mRNA (A) and HCE2 mRNA (B) by Taqman probes as described in Section 2. The adult group contained 22 samples, the child group contained 34 samples and the fetal group contained 48 samples. The signals from each target were normalized based on the signal from PolII and expressed as relative levels among all samples. The data are presented as mean ± S.D. (*) Statistical significance at $p < 0.05$, (**) statistical significance at $p < 0.001$.

was the same in the fetal and child groups and higher than that in the adult group (21- versus 4-fold) (Table 2).

We next examined whether the expression of carboxylesterases is age-related within a group. The levels of mRNA were plotted against age or gestation days, and the correlation coefficients were computed. The adult group showed no clear correlation for either HCE1 or HCE2 (data not shown). In the fetal samples, the level of HCE2 but not HCE1 mRNA was

Table 2 – Relative mRNA levels of carboxylesterases *HCE1* and *HCE2* in fetuses, children (0–10 years old) and adults (≥18).

Group	n	Minimum	Maximum	Variability	Mean	S.D.	CV (%)
Fetus-HCE1	48	0.07	30.15	431 (fold)	3.32	5.70	172
Child-HCE1	34	12.18	2657.77	218	711.47	638.51	90
Adult-HCE1	22	225.50	2659.61	12	1059.59	644.92	61
Fetus-HCE2	48	0.20	4.28	21	1.63	1.36	91
Child-HCE2	34	7.00	148.78	21	65.82	34.90	53
Adult-HCE2	22	39.89	168.66	4	89.87	34.83	39

Abbreviations: S.D.: standard deviation; CV: coefficient of variation.

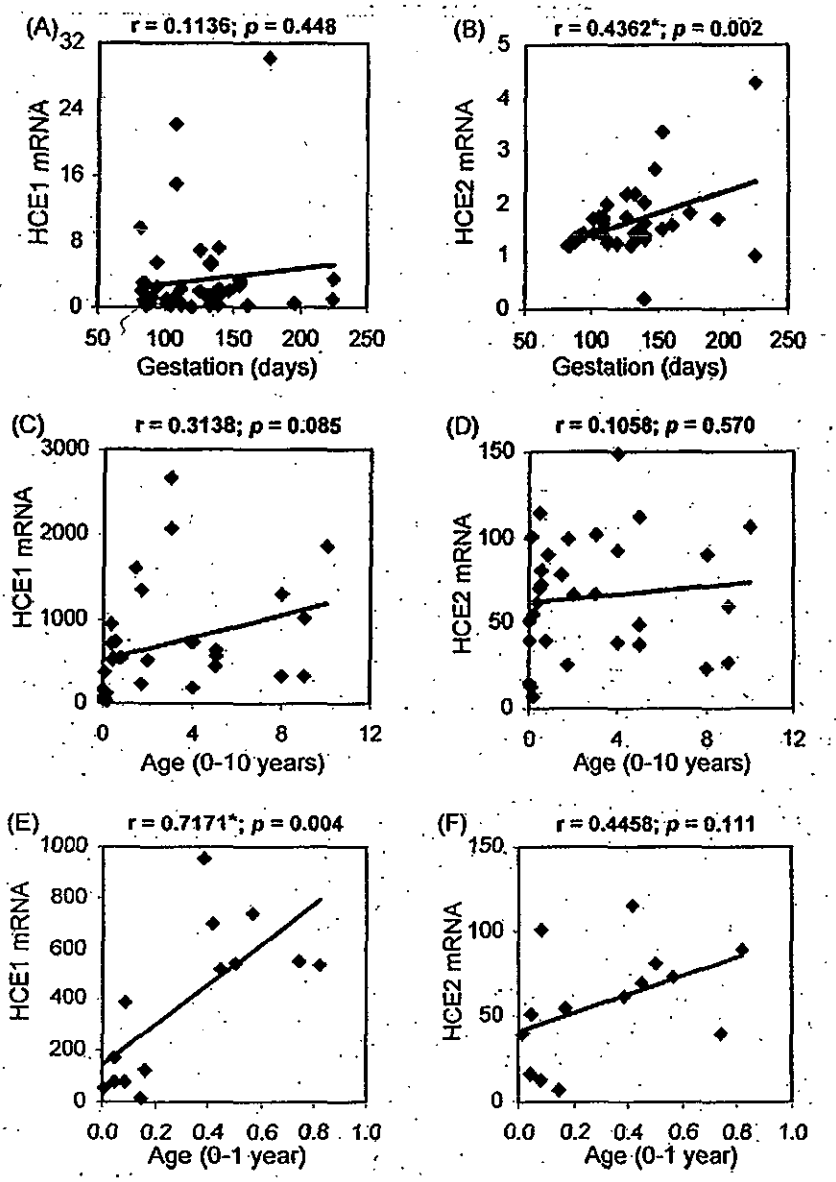

Fig. 2 – Age-related expression of HCE1 and HCE2. The data from Fig. 1 were plotted against age with SPSS version 16. (A) Correlation of HCE1 mRNA with gestation days. (B) Correlation of HCE2 mRNA with gestation days. (C) Correlation of HCE1 mRNA with age in the child group (0–10 years old). (D) Correlation of HCE2 mRNA with age in the child group (0–10 years old). (E) Correlation of HCE1 mRNA with age in the sub-child group (0–1-year-old). (F) Correlation of HCE2 mRNA with age in the sub-child group (0–1-year-old), (*) statistical significance ($p < 0.05$).

significantly correlated with age (Fig. 2A and B). In contrast, the child group showed better correlation with age on HCE1 than HCE2 mRNA, although neither correlation reached the level of statistical significance (Fig. 2C and D). To gain additional information on age-related expression, correlation analysis was performed on the samples from donors under one year old (0–1 year). In this sub-group, much improved correlation was observed on both HCE1 and HCE2 with a p-value of 0.004 and 0.111, respectively (Fig. 2E and F).

3.2. *Inter-individual variability in carboxylesterase proteins and oseltamivir hydrolysis in the child group*

We next examined whether the levels of carboxylesterase mRNA reflected the levels of corresponding proteins. RNA-microsome matched samples from 11 available pediatric-aged subjects were evaluated. Fetal matched samples were not tested because of low mRNA expression and low activities towards marker substrates (described below). No RNA-microsome matched samples were available for the adult group. The microsomal samples were first analyzed by Western immunoblotting with antibody against HCE1 or HCE2, and the immunostaining intensities were quantified by the KODAK 1D Image Analysis Software. As shown in Fig. 3A, all samples contained HCE1 and HCE2 proteins, but the relative abundance varied markedly. In particular, one donor (lane 6) showed extremely low levels of both carboxylesterases (Fig. 3A). Based on the immunostaining intensities, HCE1 protein varied by ~100-fold, and HCE2 protein varied by ~20-fold. The inter-individual variability, however, was decreased

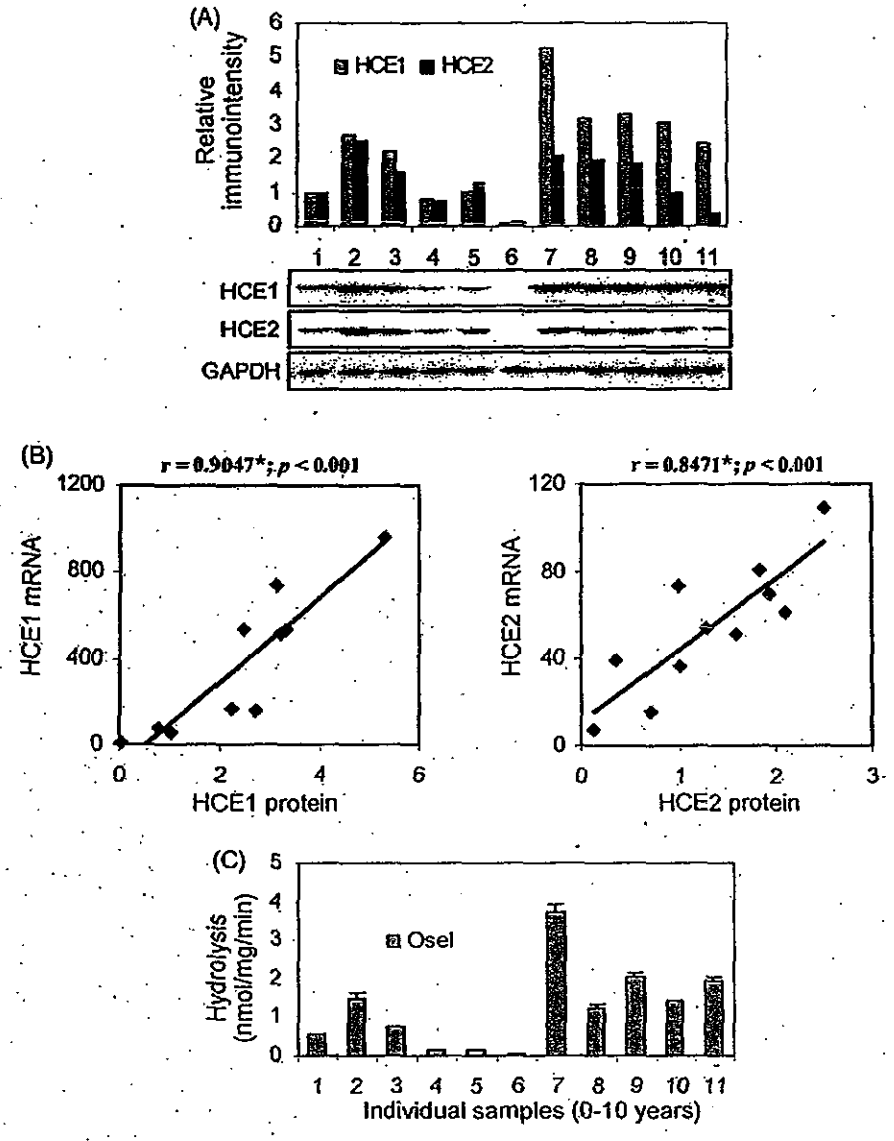

Fig. 3 – Individual variation of HCE1 and HCE2 proteins and oseltamivir hydrolysis in the child group. (A) *Western analyses.* Microsomes (1.5 μg) were resolved by 7.5% SDS-PAGE and transferred electrophoretically to nitrocellulose membranes. The blots were incubated with an antibody against HCE1, HCE2 or GAPDH and chemiluminescent substrate. The signal was captured by a KODAK Image Station 2000 and the relative intensities were quantified by the KODAK 1D Image Analysis Software. (B) *Correlation analyses.* The immunointensities of HCE1 and HCE2 were plotted against the levels of respective mRNA. The correlation coefficients and evaluations on statistical significance were performed with SPSS version 16. (*) Statistical significant ($p < 0.001$). (C) *Oseltamivir hydrolysis by individual liver samples of the child group.* Microsomes (20 μg) were incubated with oseltamivir (200 μM) at 37 °C for 10 min, and the formation of oseltamivir carboxylate was detected by LC–MS/MS. Data were assembled from three independent experiments with two injections of each experiment.

to ~8-fold for both carboxylesterases when the data-point (lane 6) was eliminated. For both HCE1 and HCE2, the mRNA levels were correlated significantly with the levels of respective proteins ($p < 0.001$) (Fig. 3B). The HCE1 matched samples had a correlation coefficient of 0.9047, and the HCE2 matched samples had a slightly lower correlation coefficient (0.8471) (Fig. 3B).

The large individual variability in carboxylesterase protein pointed to the possibility of marked differences in the metabolism of therapeutic agents and other xenobiotics. To directly test this possibility, the anti-influenza viral agent oseltamivir (an ester prodrug) was incubated with individual donor samples (Fig. 3A), and the hydrolysis was monitored. As shown in Fig. 3C, all samples hydrolyzed this anti-viral agent, and the overall hydrolysis varied by 127-fold. Such a large inter-individual variability was in agreement with the variation in the abundance of HCE1 (Fig. 3A), which has been shown to catalyze the hydrolysis of oseltamivir (3). As expected, sample 6 (lane 6) contained the lowest HCE1 protein and showed the lowest hydrolytic activity toward oseltamivir. Conversely, sample 7 (lane 7) contained the highest level of HCE1 protein and was the most active toward this anti-viral

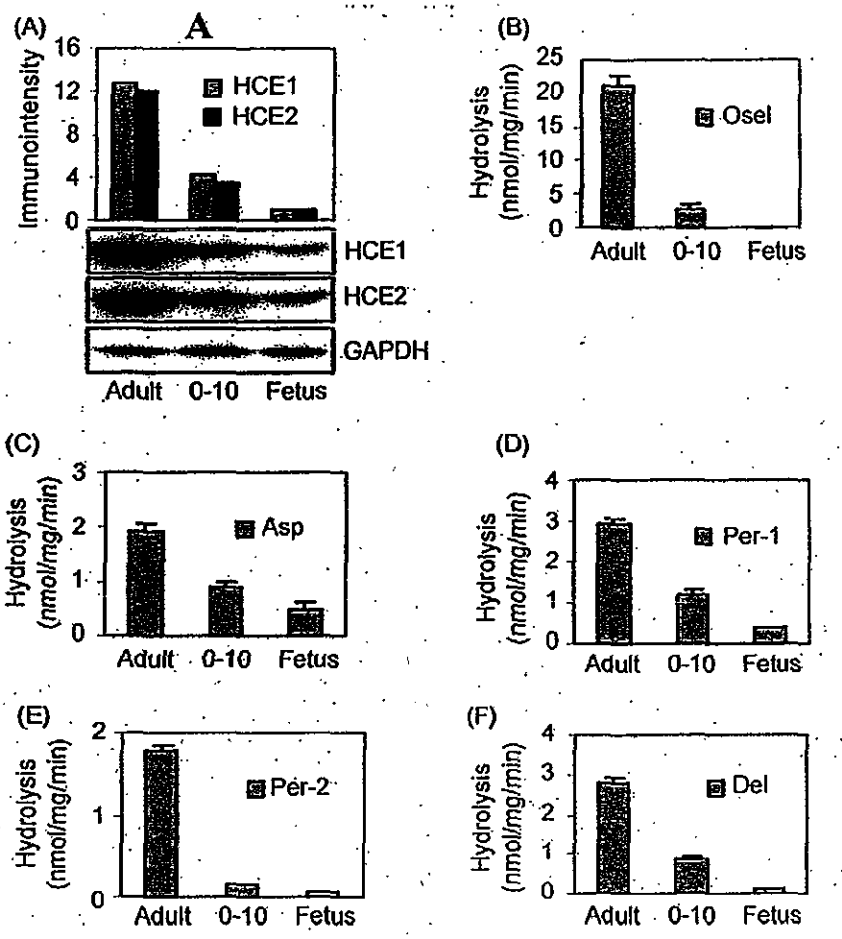

Fig. 4 – Hydrolysis of oseltamivir, aspirin, deltamethrin and permethrin. (A) *Western analysis of pooled samples for various groups.* Microsomes (1.5 μg) pooled from the adult, child and fetal group were analyzed by Western blotting and the immunostaining intensities were quantified by the KODAK 1D Image Analysis Software. (B) *Hydrolysis of oseltamivir by pooled microsomes.* Microsomes (20 μg) from various age groups were incubated with oseltamivir (200 μM) at 37 °C for 10 min, and the formation of oseltamivir carboxylate was detected by LC–MS/MS. (C) *Hydrolysis of aspirin by pooled microsomes.* Microsomes (80 μg) from various age groups were incubated with aspirin (1 mM) at 37 °C for 60 min, and the formation of salicylic acid was detected by HPLC. (D and E) *Hydrolysis of permethrin by pooled microsomes.* Microsomes (50 μg) from various age groups were incubated with permethrin (100 μM) at 37 °C for 60 min, and the disappearance of the parent compounds was detected by HPLC. Permethrin contained a mixture of *cis*- and *trans*-isomers at a ratio of 46 and 52%, respectively with the *cis*-form having a retention time of 10.41 and the *trans*-form of 10.18. (F) *Hydrolysis of deltamethrin by pooled microsomes.* Microsomes (50 μg) from various age groups were incubated with deltamethrin (100 μM) at 37 °C for 60 min, and the disappearance of the parent compound was detected by HPLC. Data were assembled from three independent experiments with each experiment having two injections.

agent (Fig. 3A and C). The hydrolysis of oseltamivir among these individual samples was highly correlated with the protein level of HCE1 with a correlation coefficient of 0.9373, although samples 8 and 10 exhibited relatively lower hydrolysis compared with their relatively HCE1 contents (Fig. 3A and C).

3.3. *Hydrolysis of drugs and insecticides by liver microsomes of fetuses, children and adults*

We next extended the metabolism study to include the anti-inflammatory agent aspirin, and insecticides permethrin (*cis*- and *trans*-) and deltamethrin. In addition to their pharmacological and toxicological implication, these chemicals were chosen because they are hydrolyzed in an isoform-specific manner. Oseltamivir and deltamethrin are predominately hydrolyzed by HCE1 [3,19,20], whereas aspirin is predominately hydrolyzed by HCE2 [4]. The *cis*-form of permethrin is favorably hydrolyzed by HCE2, whereas the *trans*-form is comparably hydrolyzed by both forms. The extended metabolism study was performed with microsomes pooled from various age groups, and the microsomes were so pooled by mixing equal amount from all individuals in an age group. The pooled samples enabled comparison to be made on the overall hydrolysis of these chemicals among different age groups.

We first determined the levels of HCE1 and HCE2 in the pooled samples by Western immunoblotting. Based on the immunostaining intensities, the child group expressed ~25%

of carboxylesterases (both HCE1 and HCE2) of the adult group and the fetal group expressed less than 10% of the adult group (Fig. 4A). Overall, the magnitude of hydrolysis of these chemicals was correlated well with the relative levels of carboxylesterases in these samples (Fig. 4B–F). The adult pooled sample showed the highest activity toward all chemicals and the fetal pooled samples showed the lowest activity. Hydrolysis of aspirin and *trans*-permethrin (Per-1) by the samples pooled from the fetuses and children was slightly higher than that predicted according to their relative abundance of carboxylesterases. For example, the fetal sample contained less than 10% of carboxylesterases of the adult sample but showed 25% of aspirin hydrolysis (Fig. 4A and C). Conversely, the hydrolysis of oseltamivir, *cis*-permethrin and deltamethrin by the fetal group was less than 10% of the adult group. The precise mechanism on these discrepancies remains to be determined. On the other hand, the higher-than predicted hydrolysis, in the case of aspirin, was likely due to hydrolysis by other enzymes (highly expressed in the fetal liver) or due to polymorphic variants. In support of these possibilities, butyrylcholinesterase has been shown to hydrolyze aspirin [21], and certain polymorphic variants of HCE2 were found to differ from the wild-type enzyme in hydrolyzing this anti-platelet agent [4]. In addition, the liver expresses a third carboxylesterase [22], but it remains to be determined whether this carboxylesterase hydrolyzes these compounds (i.e., aspirin and *trans*-permethrin) and whether the expression of this carboxylesterase is developmentally regulated.

4. Discussion

Carboxylesterases constitute a class of hydrolytic enzymes that play important roles in the metabolism of therapeutic agents and detoxication of insecticides [1]. In this study, we analyzed a large number of individual liver samples for the expression patterns of HCE1 and HCE2, two human carboxylesterases predominately expressed in the liver. Overall, the adult group expressed significantly higher HCE1 and HCE2 than the child group or the fetal group. The age-related expression was confirmed on the levels of both mRNA and protein. In agreement with the expression patterns, the adult microsomes were approximately 4 times as active as the child microsomes and more than 10 times as active as the fetal microsomes in hydrolyzing a group of therapeutic agents and insecticides. Even within the same age group, a large inter-individual variability was detected in mRNA and protein levels as well as hydrolytic activity.

Although both HCE1 and HCE2 exhibited a similar expression pattern among the various age groups, there were several major differences. First, HCE1 exhibited much greater inter-group and inter-individual variability than HCE2. For example, based on the values of the means, the adult group displayed a 319-fold higher level in HCE1 mRNA compared with the fetal group. In contrast, these two groups showed only a 55-fold difference in the level of HCE2 mRNA (Fig. 1 and Table 2). Likewise, the adult group showed a 430-fold inter-individual variability in HCE1 mRNA (ratio between maximum over minimum), in contrast, only a 21-fold difference in HCE2 mRNA was detected in the same group (Table 2). Second, HCE1 displayed better age-related expression than HCE2 in the child group with correlation coefficients of 0.3138 and 0.1058, respectively (Fig. 2C and D). In contrast, HCE2 displayed better correlation in the fetal group with correlation coefficients of 0.4362 and 0.1136, respectively (Fig. 2A and B).

The large inter-individual variability, particularly in the fetal and children groups, was likely an outcome coordinated by multiple mechanisms. In this study, we have shown that the adult group expressed the highest levels of HCE1 and HCE2 followed by the child group, and the fetal group expressed the lowest levels of both enzymes (Fig. 1 and Table 2). Such age-related expression patterns were confirmed by RT-qPCR and Western analyses (Figs. 1, 3 and 4) and established that developmental regulation is involved in the expression of HCE1 and HCE2. However, the correlation with age in many cases was only moderate at the most and did not reach the levels of statistical significance (Fig. 2C and F). Although the precise mechanisms remain to be determined, the lack of strong correlation with age in these groups was likely due to complicated factors such as the administration of therapeutic agents and disease conditions. We have previously reported that pathological condition and therapeutic agents markedly altered the expression of HCE1 and HCE2 [6,8]. Interleukin-6, a cytokine usually elevated during inflammation, profoundly suppressed the expression of both HCE1 and HCE2 [8]. Consistent with the suppression of carboxylesterases by cytokines, patients with elevated cytokine conditions such as liver cirrhosis had much lower capacity of hydrolyzing ester drugs such as perindopril, a non-sulphydryl angiotensin converting enzyme inhibitor [23,24].

The significantly lower level of HCE1 in the child group, compared with the adult group, provides a molecular explanation to the large pharmacokinetic difference in oseltamivir between these two groups. In this study, the sample pooled from the children was only ~15% as active as the sample pooled from the adults in hydrolyzing oseltamivir (Fig. 4C). Consistent with the in vitro metabolism, children under 12 years old reportedly produced only approximately half of the hydrolytic metabolite produced by adults [25]. Apparently the low level production of oseltamivir carboxylate in children was likely due to ineffective hydrolysis of the parent drug and higher clearance of the metabolite. Furthermore, we have shown that individual samples in the child group varied by as many as 127-fold in oseltamivir hydrolysis (Fig. 4A). Pharmacokinetic studies in children, however, did not detect such a large inter-individual variation in the production of hydrolytic metabolite of oseltamivir [25,26]. One explanation is that the frequency with an extremely low expression level of HCE1 is rare in the general population, and the pharmacokinetic studies were performed in 24 or fewer children [25,26]. Indeed, there was a reported rare case that an adult patient with diabetes mellitus had only 1–2% capacity of normal people in hydrolyzing clopidogrel based on the values of the means and standard deviations [27]. Like oseltamivir, clopidogrel is a substrate of HCE1 [3]. Ineffective hydrolysis of oseltamivir, on the other hand, likely leads to increased concentration in the brain. Some patients taking oseltamivir reportedly developed neurobehavioral changes [28], although a direct link remains to be established between the developed neurotoxiciy and the use of oseltamivir.

In contrast to oseltamivir, pyrethroids have long been recognized to exert neurotoxicity [29]. As a class of the most used insecticides in the world, both the general population and workers have a high risk to be exposed to these insecticides. Epidemiological studies have shown that the exposure level, in some cases, can be high [30,31]. Pyrethroid insecticides are generally considered safe to mammals, because they are rapidly eliminated by carboxylesterases. In this study, we have shown that the fetuses and children hydrolyzed pyrethroids at a rate of only ~20% or lower of the adults (Fig. 4D–F), suggesting their vulnerability to pyrethroids-induced toxicity. In support of this notion, neonatal rats were reportedly 17 times as sensitive as adult rats to cypermethrin [12]. Neurotoxicity induced by pyrethroids appears to cause irreversible damage. Prenatal exposure to deltamethrin, for example, led to a deficit in locomotor activity of offspring post-natally at 9 weeks [32]. In humans, micromolar concentrations were reported in the meconium [33]. This is particularly of relevance as fetuses have only limited capacity of hydrolytic detoxication as described in this report.

In summary, our work points to several important conclusions. First, the expression of both HCE1 and HCE2 increases with age, establishing that their expression is developmentally regulated and that fetuses and children generally have lower capacity of hydrolytic metabolism than adults. Second, there is a large inter-individual variability in the expression of these enzymes, particularly in the fetal and child groups. It is likely that the expression of HCE1 and HCE2 in these age groups is subjected to non-developmental regulation with high sensitivity (e.g., xenobiotic regulation). Carboxylesterases are recognized to play important roles in drug metabolism and insecticide detoxication. The findings on the large variability among different age groups or even within the same age group have important pharmacological and toxicological implications, particularly in relation to altered pharmacokinetics of ester drugs in children and vulnerability of fetuses and children to insecticides such as pyrethroids.

REFERENCES

[1] Satoh T, Hosokawa M. Structure, function and regulation of carboxylesterases. Chem Biol Interact 2006;162:195–211.

[2] Schwer H, Langmann T, Daig R, Becker A, Aslanidis C, Schmitz G. Molecular cloning and characterization of a novel putative carboxylesterase, present in human intestine and liver. Biochem Biophys Res Commun 1997;233:117–20.

[3] Shi D, Yang J, Yang D, LeCluyse EL, Black C, You L, et al. Anti-influenza prodrug oseltamivir is activated by carboxylesterase human carboxylesterase 1, and the activation is inhibited by antiplatelet agent clopidogrel. J Pharmacol Exp Ther 2006;319:1477–84.

[4] Tang M, Mukundan M, Yang J, Charpentier N, LeCluyse EL, Black C, et al. Antiplatelet agents aspirin and clopidogrel are hydrolyzed by distinct carboxylesterases, and clopidogrel is transesterificated in the presence of ethyl alcohol. J Pharmacol Exp Ther 2006;319:1467–76.

[5] Wu MH, Yan B, Humerickhouse R, Dolan ME. Irinotecan activation by human carboxylesterases in colorectal adenocarcinoma cells. Clin Cancer Res 2002;8:2696–700.

[6] Zhu W, Song L, Zhang H, Matoney L, LeCluyse E, Yan B. Dexamethasone differentially regulates expression of carboxylesterase genes in humans and rats. Drug Metab Dispos 2000;28:186–91.

[7] Morgan EW, Yan B, Greenway D, Parkinson A. Regulation of two rat liver microsomal carboxylesterase isozymes: species differences, tissue distribution and the effects of age, sex and xenobiotic treatment of rats. Arch Biochem Biophys 1994;315:514–26.

[8] Yang J, Shi D, Yang D, Song X, Yan B. Interleukin-6 suppresses the expression of carboxylesterases HCE1 and HCE2 through transcriptional repression. Mol Pharmacol 2007;72:686–94.

[9] Oxford JS, Mann A, Lambkin R. A designer drug against influenza: the NA inhibitor oseltamivir (Tamiflu). Expert Rev Anti Infect Ther 2003;1:337–42.

[10] Anand SS, Kim KB, Padilla S, Muralidhara S, Kim HJ, Fisher JW, et al. Ontogeny of hepatic and plasma metabolism of deltamethrin in vitro: role in age-dependent acute neurotoxicity. Drug Metab Dispos 2006;34:389–97.

[11] Pope CN, Chakraborti TK, Chapman ML, Farrar JD, Arthun D. Comparison of in vivo cholinesterase inhibition in neonatal and adult rats by three organophosphorothioate insecticides. Toxicology 1991;68:51–61.

[12] Cantalamessa F. Acute toxicity of two pyrethroids, permethrin, and cypermethrin in neonatal and adult rats. Arch Toxicol 1993;67:510–3.

[13] Sheets LP, Doherty JD, Law MW, Reiter LW, Crofton KM. Age-dependent differences in the susceptibility of rats to deltamethrin. Toxicol Appl Pharmacol 1994;126:186–90.

[14] Pope CN, Karanth S, Liu J, Yan B. Comparative carboxylesterase activities in infant and adult liver and their in vitro sensitivity to chlorpyrifos oxon. Regul Toxicol Pharm 2005;42:62–9.

[15] Vyhlidal CA, Gaedigk R, Leeder JS. Nuclear receptor expression in fetal and pediatric liver: correlation with CYP3A expression. Drug Metab Dispos 2006;34:131–7.

[16] Wortham M, Czerwinski M, He L, Parkinson A, Wan YJ. Expression of constitutive androstane receptor, hepatic nuclear factor 4 alpha, and P450 oxidoreductase genes determines interindividual variability in basal expression and activity of a broad scope of xenobiotic metabolism genes in the human liver. Drug Metab Dispos 2007;35:1700–10.

[17] Leeder JS, Gaedigk R, Marcucci KA, Gaedigk A, Vyhlidal CA, Schindel BP, et al. Variability of CYP3A7 expression in human fetal liver. J Pharmacol Exp Ther 2005;314:626–35.

[18] Radonić A, Thulke S, Mackay IM, Landt O, Siegert W, Nitsche A. Guideline to reference gene selection for quantitative real-time PCR. Biochem Biophys Res Commun 2004;313:856–62.

[19] Godin SJ, Scollon EJ, Hughes MF, Potter PM, DeVito MJ, Ross MK. Species differences in the in vitro metabolism of deltamethrin and esfenvalerate: differential oxidative and hydrolytic metabolism by humans and rats. Drug Metab Dispos 2006;34:1764–71.

[20] Nishi K, Huang H, Kamita SG, Kim IH, Morisseau C, Hammock BD Characterization of pyrethroid hydrolysis by the human liver carboxylesterases hCE-1 and hCE-2. Arch Biochem Biophys 2006;445:115–23.

[21] Kolarich D, Weber A, Pabst M, Stadlmann J, Teschner W, Ehrlich H, et al. Glycoproteomic characterization of butyrylcholinesterase from human plasma. Proteomics 2008;8:254–63.

[22] Sanghani SP, Quinney SK, Fredenburg TB, Davis WI, Murry DJ, Bosron WF. Hydrolysis of irinotecan and its oxidative metabolites, 7-ethyl-10-[4-N-(5-aminopentanoic acid)-1-piperidino] carbonyloxycamptothecin and 7-ethyl-10-[4-(1-piperidino)-1-amino]-carbonyloxycamptothecin, by human

carboxylesterases CES1A1, CES2, and a newly expressed carboxylesterase isoenzyme, CES3. Drug Metab Dispos 2004;32:505–11.
[23] Thiollet M, Funck-Brentano C, Grange JD, Midavaine M, Resplandy G, Jaillon P. The pharmacokinetics of perindopril in patients with liver cirrhosis. Br J Clin Pharmacol 1992;33:326–8.
[24] Eriksson AS, Gretzer C, Wallerstedt S. Elevation of cytokines in peritoneal fluid and blood in patients with liver cirrhosis. Hepatogastroenterology 2004;51:505–9.
[25] Oo C, Barrett J, Hill G, Mann J, Dorr A, Dutkowski R, et al. Pharmacokinetics and dosage recommendations for an oseltamivir oral suspension for the treatment of influenza in children. Paediatr Drugs 2001;3:229–36.
[26] Oo C, Hill G, Dorr A, Liu B, Boellner S, Ward P. Pharmacokinetics of anti-influenza prodrug oseltamivir in children aged 1–5 years. Eur J Clin Pharmacol 2003;59:411–5.
[27] Heestermans AA, van Werkum JW, Schömig E, ten Berg JM, Taubert D. Clopidogrel resistance caused by a failure to metabolize clopidogrel into its metabolites. J Thromb Haemost 2006;4:1143–5.
[28] FDA Patient Safety News (2007) Caution on Neuropsychiatric Events with Tamiflu: Show #59:http://www.accessdata.fda.gov/psn/printer.cfm?id=486.
[29] Ray DE, Fry JR. A reassessment of the neurotoxicity of pyrethroid insecticides. Pharmacol Ther 2006;111:174–93.
[30] Leng G, Kühn KH, Idel H. Biological monitoring of pyrethroids in blood and pyrethroid metabolites in urine: applications and limitations. Sci Total Environ 1997;199:173–81.
[31] Heudorf U, Angerer J. Metabolites of pyrethroid insecticides in urine specimens: current exposure in an urban population in Germany. Environ Health Perspect 2001;109:213–7.
[32] Johri A, Yadav S, Singh RL, Dhawan A, Ali M, Parmar D. Long lasting effects of prenatal exposure to deltamethrin on cerebral and hepatic cytochrome P450 s and behavioral activity in rat offspring. Eur J Pharmacol 2006;544:58–68.
[33] Ostrea Jr EM, Bielawski DM, Posecion Jr NC, Corrion M, Villanueva-Uy E, Jin Y, et al. A comparison of infant hair, cord blood and meconium analysis to detect fetal exposure to environmental pesticides. Environ Res 2008;106:277–83.

A−05 異常行動モデルとしての薬物誘発ジャンピング行動に対するタミフルの影響とその防御法に関する研究

○小野信文、牛島逸子、木村公彦
福岡大・薬・医薬品情報学

【背景と目的】タミフルを代表とする抗インフルエンザウイルス剤服用者が、異常行動の結果、事故死を起こしたことが報告され、緊急安全性情報が出された。その後この因果関係に関しては国家的研究班が組織され、調査研究が行われているが、詳細は未だ明らかでない。しかし、世界的に見れば新たなインフルエンザウイルスの出現もあり、それらの対処は急がねばならない状況と思われる。このような状況を踏まえ、我々は新たな視点から抗インフルエンザウイルス薬の欠点を補う可能性を検討した。

【実験方法】ジャンピング行動は、直径32 cmの正八角形、高さ35 cmの台に置いたマウスが薬物投与後40分間に下の床に飛び降りる行動とし、飛び降りるまでの時間と回数を（飛び降りた動物は台に戻し）測定した。尚、マウスは測定までこの測定台へ置かれたことはない。薬物の投与スケジュールは、haloperidol 0.5 mg/kg (ip) 5分後にclonidine 10mg/kg (ip)投与し、測定台へ移し測定を開始した。タミフル0.1%CMC懸濁液はhaloperidol 15分前に経口投与し、前処置薬はタミフルのさらに10分前にip投与した。

【結果並びに考察】タミフル150mg/kg、haloperidol、clonidineそれぞれ単独投与では測定時間内にジャンピング行動は全く起こさなかった。haloperidolとclonidineの併用では、0.63回/匹のジャンピング行動が見られた。このhaloperidol-clonidine誘発行動は、タミフル150mg/kgの併用により22.6回/匹と有意に増強された。このタミフルによる増強作用は、acetazolamide 20 mg/kg前処置により0.50回/匹と有意に抑制し、150 mg/kg前処置ではジャンピング行動を完全に消失させた。さらに、diazepam 0.5、1 mg/kg、valprorate 40 mg/kg、fluoxetine 5 mg/kg前処置により、タミフルによる薬物誘発ジャンピング行動は消失した。したがって、このようなジャンピング行動は、異常行動の一つの指標として有用と考えられる。現時点ではこれらの行動の発現機序は不明であるが、各種中枢神経伝達物質系の不均衡が関与し、抑制作用はその是正によることが示唆される。

A−06 Morphine誘発精神依存形成におけるL型高電位開口性カルシウムチャネル（HVCCs）機能亢進に対するPI 3-kinaseの関与

○芝崎真裕、黒川和宏、桂 昌司、大熊誠太郎
川崎医大・薬理学

【目的】我々は既に、精神依存の評価法である条件づけ場所嗜好性試験において、L型HVCC拮抗薬であるnifedipineにより、morphine誘発報酬効果が有意に抑制されることを報告した。一方、PI 3-kinase class IIIであるVps34はtraffickingに深く関与することが報告されていることから、morphineによるL型HVCCの発現増加に関与している可能性が考えられる。そこで本研究では、morphineによる精神依存形成過程におけるL型HVCCの発現増加を伴った機能亢進機序を、精神依存マウスおよび依存性薬物を連続曝露した初代培養大脳皮質神経細胞（神経細胞）を用いて、行動薬理学的および神経科学的観点から検討した。

【方法】Morphineによる報酬効果は条件づけ場所嗜好性試験により行った。神経細胞へのmorphineの連続曝露は、Hanks液で希釈したものを直接培養液中に添加した。[$^{45}Ca^{2+}$]$_i$流入は2分間の30 mM KCl刺激により神経細胞内へ取り込まれた放射活性を測定した。蛋白発現量はWestern blot法により解析した。

【結果および考察】Morphineによる報酬効果は、L型HVCC阻害薬（nifedipine）の前処置により完全に消失した。この時点での側坐核を含む領域および大脳皮質画分におけるL型HVCC α1cおよびα2/δ subunitならびにVps34蛋白の発現量に有意な増加が認められた。同様に、神経細胞にmorphineを連続曝露した場合に観察される30 mM KCl誘発[$^{45}Ca^{2+}$]$_i$流入の増加は、L型HVCC阻害薬の併用により完全に阻害された。また、morphineの連続曝露によりL型HVCC α1cおよびα2/δ subunitならびにVps34蛋白量の有意な増加が認められた。このα1c subunit蛋白量の増加は、PI 3-kinase阻害薬（LY294002）の併用処置により有意に減少した。以上の成績より、morphineによるL型HVCC α1c subunit蛋白発現増加機構に、Vps34が一部関与することが明らかとなった。

日本薬理学会近畿部会，第１１３回（２００８．０６．２０，岡山）